IMA Journal of Numerical Analysis (2009) **29**, 180–207
doi:10.1093/imanum/drn002
Advance Access publication on March 14, 2008

Approximation of the vibration modes of a Timoshenko curved rod of arbitrary geometry

ERWIN HERNÁNDEZ† AND ENRIQUE OTÁROLA‡
Departamento de Matemática, Universidad Técnica Federico Santa María, Casilla 110-V, Valparaíso, Chile

AND

RODOLFO RODRÍGUEZ§ AND FRANK SANHUEZA¶
GI2MA, Departamento de Ingeniería Matemática, Universidad de Concepción, Casilla 160-C, Concepción, Chile

[Received on 4 September 2007; revised on 28 December 2007]

The aim of this paper is to analyse a mixed finite-element method for computing the vibration modes of a Timoshenko curved rod with arbitrary geometry. Optimal order error estimates are proved for displacements, rotations and shear stresses of the vibration modes, as well as a double order of convergence for the vibration frequencies. These estimates are essentially independent of the thickness of the rod, which leads to the conclusion that the method is locking-free. Numerical tests are reported in order to assess the performance of the method.

Keywords: Timoshenko curved rods; finite-element method; vibration problem.

1. Introduction

It is very well known that standard finite elements applied to models of thin structures, like beams, rods, plates and shells, are subject to the so-called 'locking' phenomenon. This means that they produce very unsatisfactory results when the thickness is small with respect to the other dimensions of the structure (see, for instance, Babuška & Suri, 1992). From the point of view of the numerical analysis, this phenomenon usually reveals itself in that the *a priori* error estimates for these methods depend on the thickness of the structure in such a way that they degenerate when this parameter becomes small. To avoid locking, special methods based on reduced integration or mixed formulations have been devised and are typically used (see, for instance, Brezzi & Fortin, 1991).

Very likely, the first mathematical piece of work dealing with numerical locking and how to avoid it is the paper by Arnold (1981), where a thorough analysis for the Timoshenko beam bending model is developed. In that paper, it is proved that locking arises because of the shear terms and a locking-free method based on a mixed formulation is introduced and analysed. It is also shown that this mixed

†Email: erwin.hernandez@usm.cl
‡Email: enrique.otarola@usm.cl
§Corresponding author. Email: rodolfo@ing-mat.udec.cl
¶Email: fsanhuez@ing-mat.udec.cl

method is equivalent to the use of a reduced-order scheme for the integration of the shear terms in the primal formulation.

Subsequently, several methods to avoid locking on different models of arches were developed by Kikuchi (1982), Loula *et al.* (1987), Reddy (1988) and Reddy & Volpi (1992). The analysis of the latter was extended by Arunakirinathar & Reddy (1993) to Timoshenko rods of rather arbitrary geometry. An alternative approach to dealing with this same kind of rods was developed and analysed by Chapelle (1997), where a numerical method based on standard beam finite elements was used.

All the above references deal only with load problems. The literature devoted to the dynamic analysis of rods is less rich. There exist a few papers introducing finite-element methods and assessing their performance by means of numerical experiments (see Karami *et al.*, 1990; Litewka & Rakowski, 2001 and references therein). Papers dealing with the numerical analysis of the eigenvalue problems arising from the computation of the vibration modes for thin structures are much less frequent; among them we mention Durán *et al.* (1999, 2003), where MITC methods for computing bending vibration modes of plates were analysed. One reason for this is that the extension of mathematical results from load to vibration problems is not quite straightforward for mixed methods. Boffi *et al.* (1998, 2000) showed that eigenvalue problems for mixed formulations show peculiar features that make them substantially different from the same methods applied to the corresponding source problems. In particular, they showed that the standard inf–sup and ellipticity in the kernel conditions, which ensure convergence for the mixed formulation of source problems, are not enough to attain the same goal in the corresponding eigenvalue problem.

In this paper, we analyse a mixed finite-element method to compute the vibration modes of an elastic curved rod. For the stiffness terms, we follow the approach proposed by Arunakirinathar & Reddy (1993) for the load problem. We settle the corresponding spectral problem by including the mass terms arising from displacement and rotational inertia in the model, as proposed in Karami *et al.* (1990). Our assumptions on the rods are slightly weaker than those in these references. On the one hand, we do not assume that the Frenet basis associated with the line of cross-section centroids is a set of principal axes. On the other hand, we allow for nonconstant geometric and physical coefficients, varying smoothly along the rod. We prove that the resulting method yields an optimal order approximation of displacements, rotations and shear stresses of the vibration modes, as well as a double order of convergence for the vibration frequencies. Under mild assumptions, we also prove that the error estimates do not degenerate as the thickness becomes small, which allows us to conclude that the method is locking-free.

The outline of the paper is as follows. In Section 2, we recall the basic geometric and physical assumptions to settle the vibration problem for a Timoshenko rod of arbitrary geometry. The resulting spectral problem is shown to be well posed. Its eigenvalues and eigenfunctions are proved to converge to the corresponding ones of the limit problem as the thickness of the rod goes to zero, which corresponds to a Bernoulli-like rod model. A finite-element discretization with piecewise polynomials of arbitrary degree is introduced and analysed in Section 3. Optimal orders of convergence are proved for the eigenfunctions and the corresponding shear stresses. Finally, a double order of convergence is proved for the eigenvalues and, hence, for the vibration frequencies. All these error estimates are proved to be independent of the thickness of the rod, which allows us to conclude that the method is locking-free. In Section 4, we report several numerical tests, which allow an assessment of the performance of the lowest degree method. The experiments include different geometries and even boundary conditions not covered by the theoretical analysis. All the tests show optimal orders of convergence for all the variables. They also show that the method is completely locking-free.

2. The vibration problem for an elastic rod of arbitrary geometry

A curved rod in undeformed reference state is described by means of a smooth 3D curve, the 'line of centroids', which passes through the centroids of cross-sections of the rod. These cross-sections are initially plane and normal to the line of centroids. The curve is parameterized by its arc length $s \in \mathrm{I} := [0, L]$, L being the total length of the curve.

We recall some basic concepts and definitions; for further details see Arunakirinathar & Reddy (1993), for instance. We use standard notation for Sobolev spaces and norms.

The basis in which the equations are formulated is the 'Frenet basis' consisting of $\boldsymbol{t}$, $\boldsymbol{n}$ and $\boldsymbol{b}$, which are the tangential, normal and binormal vectors of the curve, respectively. These vectors change smoothly from point to point and form an orthogonal basis of $\mathbb{R}^3$ at each point.

Let S denote a cross-section of the rod. We denote by (η, ζ) the coordinates in the coordinate system $\{\boldsymbol{n}, \boldsymbol{b}\}$ of the plane containing S (see Fig. 1).

The geometric properties of the cross-section are determined by the following parameters (recall that the first moments of area, $\int_S \eta \mathrm{d}\eta\,\mathrm{d}\zeta$ and $\int_S \zeta \mathrm{d}\eta\,\mathrm{d}\zeta$, vanish, because the centre of coordinates is the centroid of S):

- area of S: $A := \int_S \mathrm{d}\eta\,\mathrm{d}\zeta$;
- second moments of area with respect to the axis $\boldsymbol{n}$, $I_{\boldsymbol{n}} := \int_S \zeta^2 \mathrm{d}\eta\,\mathrm{d}\zeta$, and $\boldsymbol{b}$, $I_{\boldsymbol{b}} := \int_S \eta^2 \mathrm{d}\eta\,\mathrm{d}\zeta$;
- polar moment of area: $J := \int_S (\eta^2 + \zeta^2) \mathrm{d}\eta\,\mathrm{d}\zeta = I_{\boldsymbol{n}} + I_{\boldsymbol{b}}$;
- $I_{\boldsymbol{nb}} := \int_S \eta\zeta \mathrm{d}\eta\,\mathrm{d}\zeta$.

These parameters are not necessarily constant, but they are assumed to vary smoothly along the rod. For a nondegenerate rod, A is bounded above and below far from zero. Consequently, the same happens for the area moments, $I_{\boldsymbol{n}}$, $I_{\boldsymbol{b}}$ and J.

REMARK 2.1 For any planar set S, there exists an orthogonal coordinate system, named the 'set of principal axes', such that $I_{\boldsymbol{nb}}$ vanishes when computed in these coordinates. For particularly symmetric geometries of S, for instance when the cross-section of the rod is a circle or a square, $I_{\boldsymbol{nb}}$ vanishes in any orthogonal coordinate system. However, in general, there is no reason for $\boldsymbol{n}$ and $\boldsymbol{b}$ to be principal

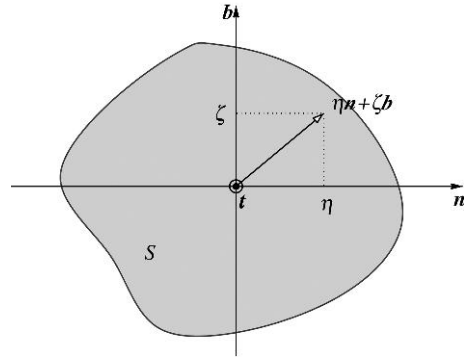

FIG. 1. Cross-section. Coordinate system.

axes, so that I_{nb} does not necessarily vanish. In any case, it is straightforward to prove that the matrix:

$$\begin{pmatrix} I_n & -I_{nb} \\ -I_{nb} & I_b \end{pmatrix}$$

is always positive definite.

Vector fields defined on the line of centroids will be always written in the Frenet basis:

$$\boldsymbol{v} = v_1\boldsymbol{t} + v_2\boldsymbol{n} + v_3\boldsymbol{b}, \quad \text{with } v_1, v_2, v_3 \colon \mathrm{I} \longrightarrow \mathbb{R}.$$

We emphasize that v_1, v_2 and v_3 are not the components of $\boldsymbol{v}$ in a fixed basis of $\mathbb{R}^3$, but in the Frenet basis $\{\boldsymbol{t}, \boldsymbol{n}, \boldsymbol{b}\}$, which changes from point to point of the curve.

Since $\boldsymbol{t}$, $\boldsymbol{n}$ and $\boldsymbol{b}$ are smooth functions of the arc-length parameter s, we have

$$\boldsymbol{v}' = v_1'\boldsymbol{t} + v_2'\boldsymbol{n} + v_3'\boldsymbol{b} + v_1\boldsymbol{t}' + v_2\boldsymbol{n}' + v_3\boldsymbol{b}'.$$

If we denote

$$\dot{\boldsymbol{v}} := v_1'\boldsymbol{t} + v_2'\boldsymbol{n} + v_3'\boldsymbol{b}, \tag{2.1}$$

then, by using the 'Frenet–Serret formulas' (see, for instance, Arunakirinathar & Reddy, 1993), we have

$$\boldsymbol{v}' = \dot{\boldsymbol{v}} + \Gamma^{\mathrm{t}}\boldsymbol{v}, \quad \text{with } \Gamma(s) := \begin{pmatrix} 0 & \kappa(s) & 0 \\ -\kappa(s) & 0 & \tau(s) \\ 0 & -\tau(s) & 0 \end{pmatrix},$$

where κ and τ are the curvature and the torsion of the rod, which are also smooth functions of s. Therefore, $\boldsymbol{v} = v_1\boldsymbol{t} + v_2\boldsymbol{n} + v_3\boldsymbol{b} \in \mathrm{H}^1(\mathrm{I})^3$ if and only if $v_i \in \mathrm{L}^2(\mathrm{I})$ and $\dot{v}_i \in \mathrm{L}^2(\mathrm{I})$, $i = 1, 2, 3$.

Since we will confine our attention to elastic rods clamped at both ends, we proceed as in Arunakirinathar & Reddy (1993) and consider

$$\mathscr{V} := \{\boldsymbol{v} \in \mathrm{L}^2(\mathrm{I})^3 : \ \dot{\boldsymbol{v}} \in \mathrm{L}^2(\mathrm{I})^3 \text{ and } \boldsymbol{v}(0) = \boldsymbol{v}(L) = \boldsymbol{0}\},$$

endowed with its natural norm

$$\|\boldsymbol{v}\|_1 := \left[\int_0^L (|\boldsymbol{v}|^2 + |\dot{\boldsymbol{v}}|^2)\mathrm{d}s\right]^{1/2};$$

namely, $\mathscr{V}$ is the space of vector fields defined on the line of centroids such that their components in the Frenet basis are in $\mathrm{H}_0^1(\mathrm{I})$.

We will systematically use in what follows the total derivative $\boldsymbol{v}' = \dot{\boldsymbol{v}} + \Gamma^{\mathrm{t}}\boldsymbol{v}$. Since $\boldsymbol{t}$, $\boldsymbol{n}$ and $\boldsymbol{b}$ are assumed to be smooth functions, $\|\boldsymbol{v}'\|_0$ is a norm on $\mathscr{V}$ equivalent to $\|\cdot\|_1$ (see Arunakirinathar & Reddy, 1993, Theorem 3.1). This is the reason why we denote $\|\cdot\|_1$ the norm of $\mathscr{V}$. However, the total derivative $\boldsymbol{v}'$ should be distinguished from the vector $\dot{\boldsymbol{v}}$ of derivatives of the components of $\boldsymbol{v}$ in the Frenet basis, as defined by (2.1).

The kinematic hypotheses of Timoshenko are used for the problem formulation. The deformation of the rod is described by the displacement of the line of centroids, $\boldsymbol{u} \in \mathbb{R}^3$, and the rotation of the cross-sections, $\boldsymbol{\theta} \in \mathbb{R}^3$. The physical properties of the rod are determined by the elastic and the shear

moduli E and G, respectively, the shear correcting factors k_1 and k_2 and the volumetric density ρ, all of them strictly positive coefficients. These coefficients are not necessarily constant; they are allowed to vary along the rod, but they are also assumed to be smooth functions of the arc length s.

We consider the problem of computing the free vibration modes of an elastic rod clamped at both ends. The variational formulation of this problem consists in finding nontrivial $(\boldsymbol{u}, \boldsymbol{\theta}) \in \mathscr{W} := \mathscr{V} \times \mathscr{V}$ and $\omega > 0$ such that

$$\int_0^L \mathbb{E}\boldsymbol{\theta}' \cdot \boldsymbol{\psi}' \mathrm{ds} + \int_0^L \mathbb{D}(\boldsymbol{u}' - \boldsymbol{\theta} \times \boldsymbol{t}) \cdot (\boldsymbol{v}' - \boldsymbol{\psi} \times \boldsymbol{t}) \mathrm{ds} = \omega^2 \left(\int_0^L \rho A \boldsymbol{u} \cdot \boldsymbol{v} \mathrm{ds} + \int_0^L \rho \mathbb{J}\boldsymbol{\theta} \cdot \boldsymbol{\psi} \, \mathrm{ds} \right)$$
$$\forall (\boldsymbol{v}, \boldsymbol{\psi}) \in \mathscr{W}, \quad (2.2)$$

where ω is the vibration frequency and $\boldsymbol{u}$ and $\boldsymbol{\theta}$ are the amplitudes of the displacements and the rotations, respectively (see Karami *et al.*, 1990). The coefficients $\mathbb{D}$, $\mathbb{E}$ and $\mathbb{J}$ are 3×3 matrices, which in the Frenet basis are written as follows:

$$\mathbb{D} := \begin{pmatrix} EA & 0 & 0 \\ 0 & k_1 GA & 0 \\ 0 & 0 & k_2 GA \end{pmatrix}, \quad \mathbb{E} := \begin{pmatrix} GJ & 0 & 0 \\ 0 & EI_{\boldsymbol{n}} & -EI_{\boldsymbol{nb}} \\ 0 & -EI_{\boldsymbol{nb}} & EI_{\boldsymbol{b}} \end{pmatrix} \quad \text{and} \quad \mathbb{J} := \begin{pmatrix} J & 0 & 0 \\ 0 & I_{\boldsymbol{n}} & -I_{\boldsymbol{nb}} \\ 0 & -I_{\boldsymbol{nb}} & I_{\boldsymbol{b}} \end{pmatrix}.$$

In Karami *et al.* (1990), as in most references (Arunakirinathar & Reddy, 1993; Chapelle, 1997, for instance), the Frenet basis is assumed to be a set of principal axes, so that $I_{\boldsymbol{nb}} = 0$ and the above three matrices are diagonal. We do not make this assumption in this paper.

REMARK 2.2 The above vibration problem can be formally obtained from the 3D linear elasticity equations as follows: according to the Timoshenko hypotheses, the admissible displacements at each point $\eta \boldsymbol{n} + \zeta \boldsymbol{b} \in S$ (see Fig. 1) are of the form $\boldsymbol{u} + \boldsymbol{\theta} \times (\eta \boldsymbol{n} + \zeta \boldsymbol{b})$, with $\boldsymbol{u}$, $\boldsymbol{\theta}$, $\boldsymbol{n}$ and $\boldsymbol{b}$ being functions of the arc-length coordinate s. Test and trial displacements of this form are taken in the variational formulation of the linear elasticity equations for the vibration problem of the 3D rod. By integrating over the cross-sections and multiplying the shear terms by correcting factors k_1 and k_2, one arrives at problem (2.2).

It is well known that standard finite-element methods applied to equations like (2.2) are subject to 'numerical locking': they lead to unacceptably poor results for very thin structures, unless the mesh size is excessively small. This phenomenon is due to the different scales with respect to the thickness of the rod of the two terms on the left-hand side of this equation. An adequate framework for the mathematical analysis of locking is obtained by rescaling the equations in order to obtain a family of problems with a well-posed limit as the thickness becomes infinitely small.

With this purpose, we introduce the following nondimensional parameter, characteristic of the thickness of the rod:

$$d^2 := \frac{1}{L} \int_0^L \frac{J}{AL^2} \, \mathrm{ds}.$$

If we define

$$\lambda := \frac{\omega^2 \rho}{d^2}, \quad \widehat{\mathbb{D}} := \frac{1}{d^2}\mathbb{D}, \quad \widehat{\mathbb{E}} := \frac{1}{d^4}\mathbb{E}, \quad \widehat{\mathbb{J}} := \frac{1}{d^4}\mathbb{J} \quad \text{and} \quad \widehat{A} := \frac{A}{d^2},$$

problem (2.2) can be equivalently written as follows: find nontrivial $(\boldsymbol{u}, \boldsymbol{\theta}) \in \mathscr{W}$ and $\lambda \in \mathbb{R}$ such that

$$\int_0^L \widehat{\mathbb{E}}\boldsymbol{\theta}' \cdot \boldsymbol{\psi}' \mathrm{d}s + \frac{1}{d^2} \int_0^L \widehat{\mathbb{D}}(\boldsymbol{u}' - \boldsymbol{\theta} \times \boldsymbol{t}) \cdot (\boldsymbol{v}' - \boldsymbol{\psi} \times \boldsymbol{t}) \mathrm{d}s = \lambda \left(\int_0^L \widehat{A}\boldsymbol{u} \cdot \boldsymbol{v} \mathrm{d}s + d^2 \int_0^L \widehat{\mathbb{J}}\boldsymbol{\theta} \cdot \boldsymbol{\psi} \, \mathrm{d}s \right), \quad \forall (\boldsymbol{v}, \boldsymbol{\psi}) \in \mathscr{W}. \tag{2.3}$$

The values of interest of d are obviously bounded above, so we restrict our attention to $d \in (0, d_{\max}]$. The coefficients of the matrices $\widehat{\mathbb{D}}$, $\widehat{\mathbb{E}}$ and $\widehat{\mathbb{J}}$, as well as $\widehat{A}$, are assumed to be functions of s which do not vary with d. This corresponds to considering a family of problems where the size of the cross-sections are uniformly scaled by d at all point of the line of centroids, while their shapes as well as the geometry of the curve and the material properties remain fixed.

REMARK 2.3 Matrices $\widehat{\mathbb{D}}$, $\widehat{\mathbb{E}}$ and $\widehat{\mathbb{J}}$ are positive definite for all $s \in \mathrm{I}$, the last two because of Remark 2.1. Moreover, since all the coefficients are continuous functions of s, the eigenvalues of each of these matrices are uniformly bounded below away from zero for all $s \in \mathrm{I}$.

REMARK 2.4 The eigenvalues λ of problem (2.3) are strictly positive because of the symmetry and the positiveness of the bilinear forms on its left- and right-hand sides. The positiveness of the latter is a straightforward consequence of Remark 2.3, whereas that of the former follows from the ellipticity of this bilinear form in $\mathscr{W}$. This can be proved by using Remark 2.3 again and proceeding as in the proof of Lemma 3.4 (a) from Arunakirinathar & Reddy (1993), where the same result appears for particular constant coefficients (see also Chapelle, 1997, Proposition 1).

We introduce the scaled shear stress $\boldsymbol{\gamma} := \frac{1}{d^2}\widehat{\mathbb{D}}(\boldsymbol{u}' - \boldsymbol{\theta} \times \boldsymbol{t})$ to rewrite problem (2.3) as follows:

$$(\widehat{\mathbb{E}}\boldsymbol{\theta}', \boldsymbol{\psi}') + (\boldsymbol{\gamma}, \boldsymbol{v}' - \boldsymbol{\psi} \times \boldsymbol{t}) = \lambda[(\widehat{A}\boldsymbol{u}, \boldsymbol{v}) + d^2(\widehat{\mathbb{J}}\boldsymbol{\theta}, \boldsymbol{\psi})] \quad \forall (\boldsymbol{v}, \boldsymbol{\psi}) \in \mathscr{W}, \tag{2.4}$$

$$\boldsymbol{\gamma} = \frac{1}{d^2}\widehat{\mathbb{D}}(\boldsymbol{u}' - \boldsymbol{\theta} \times \boldsymbol{t}), \tag{2.5}$$

where $(\cdot, \cdot)$ denotes the $\mathrm{L}^2(\mathrm{I})^3$ inner product.

To analyse this problem, we introduce the operator

$$T\colon \mathrm{L}^2(\mathrm{I})^3 \times \mathrm{L}^2(\mathrm{I})^3 \longrightarrow \mathrm{L}^2(\mathrm{I})^3 \times \mathrm{L}^2(\mathrm{I})^3,$$

defined by $T(\boldsymbol{f}, \boldsymbol{\phi}) := (\boldsymbol{u}, \boldsymbol{\theta})$, where $(\boldsymbol{u}, \boldsymbol{\theta}) \in \mathscr{W}$ is the solution of the associated load problem

$$(\widehat{\mathbb{E}}\boldsymbol{\theta}', \boldsymbol{\psi}') + (\boldsymbol{\gamma}, \boldsymbol{v}' - \boldsymbol{\psi} \times \boldsymbol{t}) = (\widehat{A}\boldsymbol{f}, \boldsymbol{v}) + d^2(\widehat{\mathbb{J}}\boldsymbol{\phi}, \boldsymbol{\psi}) \quad \forall (\boldsymbol{v}, \boldsymbol{\psi}) \in \mathscr{W}, \tag{2.6}$$

$$\boldsymbol{\gamma} = \frac{1}{d^2}\widehat{\mathbb{D}}(\boldsymbol{u}' - \boldsymbol{\theta} \times \boldsymbol{t}). \tag{2.7}$$

Taking into account that (2.7) can be equivalently written as follows:

$$(\boldsymbol{u}' - \boldsymbol{\theta} \times \boldsymbol{t}, \boldsymbol{q}) - d^2(\widehat{\mathbb{D}}^{-1}\boldsymbol{\gamma}, \boldsymbol{q}) = 0 \quad \forall \boldsymbol{q} \in \mathscr{Q} := \mathrm{L}^2(\mathrm{I})^3,$$

we note that the load problem falls with in the framework of the mixed formulations considered in Brezzi & Fortin (1991). In this reference, the results from Arnold (1981) are extended to cover this kind of problem. In particular, according to Brezzi & Fortin (1991, Theorem II.1.2), to prove the well posedness it is enough to verify the classical properties of mixed problems:

(i) ellipticity in the kernel: $\exists\,\alpha > 0$ such that

$$(\widehat{\mathbb{E}}\boldsymbol{\psi}', \boldsymbol{\psi}') \geqslant \alpha(\|\boldsymbol{v}\|_1^2 + \|\boldsymbol{\psi}\|_1^2) \quad \forall\,(\boldsymbol{v}, \boldsymbol{\psi}) \in \boldsymbol{\mathcal{W}}_0,$$

where $\boldsymbol{\mathcal{W}}_0 := \{(\boldsymbol{v}, \boldsymbol{\psi}) \in \boldsymbol{\mathcal{W}} : \boldsymbol{v}' - \boldsymbol{\psi} \times \boldsymbol{t} = 0 \ \text{ in I}\}$;

(ii) inf–sup condition: $\exists\,\beta > 0$ such that

$$\sup_{(\boldsymbol{0},\boldsymbol{0})\neq(\boldsymbol{v},\boldsymbol{\psi})\in\boldsymbol{\mathcal{W}}} \frac{(\boldsymbol{q}, \boldsymbol{v}' - \boldsymbol{\psi} \times \boldsymbol{t})}{\|\boldsymbol{v}\|_1 + \|\boldsymbol{\psi}\|_1} \geqslant \beta\|\boldsymbol{q}\|_0 \quad \forall\,\boldsymbol{q} \in \boldsymbol{\mathcal{Q}}.$$

Property (i) has been proved in Arunakirinathar & Reddy (1993, Lemma 3.6) for $\widehat{\mathbb{E}}$ being the identity matrix. The extension to $\widehat{\mathbb{E}}$ positive definite uniformly in s is quite straightforward. Property (ii) has been proved in Arunakirinathar & Reddy (1993, Lemma 3.7). An alternative, simpler proof of an equivalent inf–sup condition appears in Chapelle (1997, Proposition 2).

Therefore, according to Brezzi & Fortin (1991, Theorem II.1.2), problem (2.6)–(2.7) has a unique solution $(\boldsymbol{u}, \boldsymbol{\theta}, \boldsymbol{\gamma}) \in \boldsymbol{\mathcal{W}} \times \boldsymbol{\mathcal{Q}}$ and this solution satisfies

$$\|\boldsymbol{u}\|_1 + \|\boldsymbol{\theta}\|_1 + \|\boldsymbol{\gamma}\|_0 \leqslant C(\|\boldsymbol{f}\|_0 + d^2\|\boldsymbol{\phi}\|_0). \tag{2.8}$$

Here and what follows, C denotes a strictly positive constant, not necessarily the same at each occurrence, but always independent of d and of the mesh size h, which will be introduced in Section 3.

Because of the estimate above and the compact embedding $\mathrm{H}^1(\mathrm{I}) \hookrightarrow \mathrm{L}^2(\mathrm{I})$, the operator T is compact. Moreover, by substituting (2.7) into (2.6), from the symmetry of the resulting bilinear forms, it is immediate to show that T is self-adjoint with respect to the 'weighted' $\mathrm{L}^2(\mathrm{I})^3 \times \mathrm{L}^2(\mathrm{I})^3$ inner product in the right-hand side of (2.6). Therefore, apart from $\mu = 0$, the spectrum of T consists of a sequence of finite-multiplicity real eigenvalues converging to zero, all with ascent one.

Note that λ is a nonzero eigenvalue of problem (2.3) if and only if $\mu := 1/\lambda$ is a nonzero eigenvalue of T, with the same multiplicity and corresponding eigenfunctions. Recall that these eigenvalues are strictly positive (cf. Remark 2.4).

Next, we define T_0 by means of the limit problem of (2.6)–(2.7) as $d \to 0$:

$$T_0\colon \mathrm{L}^2(\mathrm{I})^3 \times \mathrm{L}^2(\mathrm{I})^3 \longrightarrow \mathrm{L}^2(\mathrm{I})^3 \times \mathrm{L}^2(\mathrm{I})^3,$$

where $T_0(\boldsymbol{f}, \boldsymbol{\phi}) := (\boldsymbol{u}_0, \boldsymbol{\theta}_0) \in \boldsymbol{\mathcal{W}}$ is such that there exists $\boldsymbol{\gamma}_0 \in \boldsymbol{\mathcal{Q}}$ satisfying:

$$(\widehat{\mathbb{E}}\boldsymbol{\theta}_0', \boldsymbol{\psi}') + (\boldsymbol{\gamma}_0, \boldsymbol{v}' - \boldsymbol{\psi} \times \boldsymbol{t}) = (\widehat{A}\boldsymbol{f}, \boldsymbol{v}) \quad \forall\,(\boldsymbol{v}, \boldsymbol{\psi}) \in \boldsymbol{\mathcal{W}}, \tag{2.9}$$

$$\boldsymbol{u}_0' - \boldsymbol{\theta}_0 \times \boldsymbol{t} = \boldsymbol{0}. \tag{2.10}$$

The above-mentioned existence and uniqueness results cover this problem as well.

Our next goal is to prove that T converges to T_0 as d goes to zero. With this purpose, we will use the following *a priori* estimates for the solutions of problems (2.6)–(2.7) and (2.9)–(2.10), whose proof is based on the same arguments as those used to prove Proposition 3 in Chapelle (1997): if $\boldsymbol{f}, \boldsymbol{\phi} \in \mathrm{H}^{k-2}(\mathrm{I})^3$, $k \geqslant 2$, then

$$\|\boldsymbol{u}\|_k + \|\boldsymbol{\theta}\|_k + \|\boldsymbol{\gamma}\|_{k-1} \leqslant C(\|\boldsymbol{f}\|_{k-2} + d^2\|\boldsymbol{\phi}\|_{k-2}), \tag{2.11}$$

$$\|\boldsymbol{u}_0\|_k + \|\boldsymbol{\theta}_0\|_k + \|\boldsymbol{\gamma}_0\|_{k-1} \leqslant C\|\boldsymbol{f}\|_{k-2}. \tag{2.12}$$

In the following lemma and thereafter, $\|\cdot\|_1$ denotes the natural product norm in $\boldsymbol{\mathcal{W}} = \boldsymbol{\mathcal{V}} \times \boldsymbol{\mathcal{V}}$.

LEMMA 2.5 There exists a constant $C > 0$, independent of d, such that

$$\|(T - T_0)(\boldsymbol{f}, \boldsymbol{\phi})\|_1 \leqslant Cd(\|\boldsymbol{f}\|_0 + d\|\boldsymbol{\phi}\|_0) \quad \forall \boldsymbol{f}, \boldsymbol{\phi} \in \mathrm{L}^2(\mathrm{I})^3.$$

Proof. Given $\boldsymbol{f}, \boldsymbol{\phi} \in \mathrm{L}^2(\mathrm{I})^3$, let $(\boldsymbol{u}, \boldsymbol{\theta}) := T(\boldsymbol{f}, \boldsymbol{\phi})$ and $(\boldsymbol{u}_0, \boldsymbol{\theta}_0) := T_0(\boldsymbol{f}, \boldsymbol{\phi})$. Subtracting (2.9) from (2.6) and (2.10) from (2.7), we have

$$(\widehat{\mathbb{E}}(\boldsymbol{\theta}' - \boldsymbol{\theta}_0'), \boldsymbol{\psi}') + (\boldsymbol{\gamma} - \boldsymbol{\gamma}_0, \boldsymbol{v}' - \boldsymbol{\psi} \times \boldsymbol{t}) = d^2(\widehat{\mathbb{J}}\boldsymbol{\phi}, \boldsymbol{\psi}) \quad \forall (\boldsymbol{v}, \boldsymbol{\psi}) \in \mathscr{W}, \tag{2.13}$$

$$\boldsymbol{\gamma} = \frac{1}{d^2}\widehat{\mathbb{D}}(\boldsymbol{u}' - \boldsymbol{u}_0' - (\boldsymbol{\theta} - \boldsymbol{\theta}_0) \times \boldsymbol{t}). \tag{2.14}$$

Taking $\boldsymbol{\psi} = \boldsymbol{\theta} - \boldsymbol{\theta}_0$ and $\boldsymbol{v} = \boldsymbol{u} - \boldsymbol{u}_0$, we obtain

$$(\widehat{\mathbb{E}}(\boldsymbol{\theta}' - \boldsymbol{\theta}_0'), \boldsymbol{\theta}' - \boldsymbol{\theta}_0') = d^2(\widehat{\mathbb{J}}\boldsymbol{\phi}, (\boldsymbol{\theta} - \boldsymbol{\theta}_0)) - d^2(\boldsymbol{\gamma} - \boldsymbol{\gamma}_0, \boldsymbol{\gamma}).$$

Using the ellipticity of the bilinear form on the left-hand side, Cauchy–Schwarz inequality, (2.11) and (2.12), we have

$$\begin{aligned}\|\boldsymbol{\theta} - \boldsymbol{\theta}_0\|_1^2 &\leqslant Cd^2\|\boldsymbol{\phi}\|_0\|\boldsymbol{\theta} - \boldsymbol{\theta}_0\|_0 + Cd^2(\|\boldsymbol{\gamma}\|_0 + \|\boldsymbol{\gamma}_0\|_0)\|\boldsymbol{\gamma}\|_0 \\ &\leqslant Cd^2\|\boldsymbol{\phi}\|_0\|\boldsymbol{\theta} - \boldsymbol{\theta}_0\|_0 + Cd^2(\|\boldsymbol{f}\|_0 + d^2\|\boldsymbol{\phi}\|_0)\|\boldsymbol{f}\|_0,\end{aligned}$$

whence

$$\|\boldsymbol{\theta} - \boldsymbol{\theta}_0\|_1 \leqslant Cd(\|\boldsymbol{f}\|_0 + d\|\boldsymbol{\phi}\|_0). \tag{2.15}$$

On the other hand, observe that from (2.14)

$$\boldsymbol{u}' - \boldsymbol{u}_0' = d^2\widehat{\mathbb{D}}^{-1}\boldsymbol{\gamma} + (\boldsymbol{\theta} - \boldsymbol{\theta}_0) \times \boldsymbol{t}.$$

Hence, using (2.8) and Poincaré inequality, we obtain

$$\|\boldsymbol{u} - \boldsymbol{u}_0\|_1 \leqslant Cd^2(\|\boldsymbol{f}\|_0 + d\|\boldsymbol{\phi}\|_0) + \|\boldsymbol{\theta} - \boldsymbol{\theta}_0\|_0,$$

which together with (2.15) allow us to end the proof. □

As a consequence of this lemma, T converges in norm to T_0 as d goes to zero. Therefore, standard properties of separation of isolated parts of the spectrum (see, for instance, Kato, 1995) yield the following result.

LEMMA 2.6 Let $\mu_0 > 0$ be an eigenvalue of T_0 of multiplicity m. Let D be any disc in the complex plane centered at μ_0 and containing no other element of the spectrum of T_0. Then, for d small enough, D contains exactly m eigenvalues of T (repeated according to their respective multiplicities). Consequently, each eigenvalue $\mu_0 > 0$ of T_0 is a limit of eigenvalues μ of T, as d goes to zero.

Moreover, for any compact subset K of the complex plane not intersecting the spectrum of T_0, there exists $d_K > 0$ such that for all $d < d_K$, K does not intersect the spectrum of T, either.

3. Finite-element discretization

Two different finite-element discretizations of the load problem for Timoshenko curved rods have been analysed in Arunakirinathar & Reddy (1993) and Chapelle (1997). The two methods differ in the variables being discretized: the components of vector fields $\boldsymbol{v}$ in the Frenet basis, v_1, v_2 and v_3, are discretized by piecewise polynomial continuous functions in the former, whereas the discretized variable is the vector field $\boldsymbol{v} = v_1\boldsymbol{t} + v_2\boldsymbol{n} + v_3\boldsymbol{b}$ in the latter. We follow the approach from Arunakirinathar & Reddy (1993).

Consider a family $\{\mathscr{T}_h\}$ of partitions of the interval I:

$$\mathscr{T}_h : \ 0 = s_0 < s_1 < \cdots < s_n = L,$$

with mesh size

$$h := \max_{j=1,\ldots,n} (s_j - s_{j-1}).$$

We define the following finite-element subspaces of $\boldsymbol{\mathscr{V}}$ and $\boldsymbol{\mathscr{Q}}$, respectively:

$$\boldsymbol{\mathscr{V}}_h := \{\boldsymbol{v} \in \boldsymbol{\mathscr{V}} : \ v_i|_{[s_{j-1},s_j]} \in \mathscr{P}_r, \ j = 1, \ldots, n, \ i = 1, 2, 3\},$$

$$\boldsymbol{\mathscr{Q}}_h := \{\boldsymbol{q} \in \boldsymbol{\mathscr{Q}} : \ q_i|_{[s_{j-1},s_j]} \in \mathscr{P}_{r-1}, \ j = 1, \ldots, n, \ i = 1, 2, 3\},$$

where v_i, $i = 1, 2, 3$, are the components of $\boldsymbol{v}$ in the Frenet basis, $\mathscr{P}_k$ are the spaces of polynomials of degree lower than or equal to k and $r \geqslant 1$.

Let $\boldsymbol{\mathscr{W}}_h := \boldsymbol{\mathscr{V}}_h \times \boldsymbol{\mathscr{V}}_h$. The following is the discrete vibration problem in mixed form: find nontrivial $(\boldsymbol{u}_h, \boldsymbol{\theta}_h, \boldsymbol{\gamma}_h) \in \boldsymbol{\mathscr{W}}_h \times \boldsymbol{\mathscr{Q}}_h$ and $\lambda_h \in \mathbb{R}$ such that

$$(\widehat{\mathbb{E}}\boldsymbol{\theta}_h', \boldsymbol{\psi}_h') + (\boldsymbol{\gamma}_h, \boldsymbol{v}_h' - \boldsymbol{\psi}_h \times \boldsymbol{t}) = \lambda_h[(\widehat{A}\boldsymbol{u}_h, \boldsymbol{v}_h) + d^2(\widehat{\mathbb{J}}\boldsymbol{\theta}_h, \boldsymbol{\psi}_h)] \quad \forall\, (\boldsymbol{v}_h, \boldsymbol{\psi}_h) \in \boldsymbol{\mathscr{W}}_h, \tag{3.1}$$

$$(\boldsymbol{u}_h' - \boldsymbol{\theta}_h \times \boldsymbol{t}, \boldsymbol{q}_h) - d^2(\widehat{\mathbb{D}}^{-1}\boldsymbol{\gamma}_h, \boldsymbol{q}_h) = 0 \quad \forall\, \boldsymbol{q}_h \in \boldsymbol{\mathscr{Q}}_h. \tag{3.2}$$

In the same manner as in the continuous case, we introduce the operator

$$T_h : \ \mathrm{L}^2(\mathrm{I})^3 \times \mathrm{L}^2(\mathrm{I})^3 \longrightarrow \mathrm{L}^2(\mathrm{I})^3 \times \mathrm{L}^2(\mathrm{I})^3,$$

defined by $T_h(\boldsymbol{f}, \boldsymbol{\phi}) := (\boldsymbol{u}_h, \boldsymbol{\theta}_h)$, where $(\boldsymbol{u}_h, \boldsymbol{\theta}_h, \boldsymbol{\gamma}_h) \in \boldsymbol{\mathscr{W}}_h \times \boldsymbol{\mathscr{Q}}_h$ is the solution of the associated discrete load problem

$$(\widehat{\mathbb{E}}\boldsymbol{\theta}_h', \boldsymbol{\psi}_h') + (\boldsymbol{\gamma}_h, \boldsymbol{v}_h' - \boldsymbol{\theta}_h \times \boldsymbol{t}) = (\widehat{A}\boldsymbol{f}, \boldsymbol{v}_h) + d^2(\widehat{\mathbb{J}}\boldsymbol{\phi}, \boldsymbol{\psi}_h) \quad \forall\, (\boldsymbol{v}_h, \boldsymbol{\psi}_h) \in \boldsymbol{\mathscr{W}}_h, \tag{3.3}$$

$$(\boldsymbol{u}_h' - \boldsymbol{\theta}_h \times \boldsymbol{t}, \boldsymbol{q}_h) - d^2(\widehat{\mathbb{D}}^{-1}\boldsymbol{\gamma}_h, \boldsymbol{q}_h) = 0 \quad \forall\, \boldsymbol{q}_h \in \boldsymbol{\mathscr{Q}}_h. \tag{3.4}$$

This problem falls with in the framework of the discrete mixed formulations considered in Brezzi & Fortin (1991, Section II.2.4). In order to apply the results from this reference, we have to verify the following classical properties, for h small enough:

(i) ellipticity in the discrete kernel: $\exists\, \alpha_* > 0$, independent of h, such that

$$(\widehat{\mathbb{E}}\boldsymbol{\psi}_h', \boldsymbol{\psi}_h') \geqslant \alpha_*(\|\boldsymbol{v}_h\|_1^2 + \|\boldsymbol{\psi}_h\|_1^2) \quad \forall\, (\boldsymbol{v}_h, \boldsymbol{\psi}_h) \in \boldsymbol{\mathscr{W}}_{0h}, \tag{3.5}$$

where $\boldsymbol{\mathscr{W}}_{0h} := \{(\boldsymbol{v}_h, \boldsymbol{\psi}_h) \in \boldsymbol{\mathscr{W}}_h : \ (\boldsymbol{q}_h, \boldsymbol{v}_h' - \boldsymbol{\psi}_h \times \boldsymbol{t}) = 0 \ \forall\, \boldsymbol{q}_h \in \boldsymbol{\mathscr{Q}}_h\}$;

(ii) discrete inf–sup condition: $\exists\, \beta_* > 0$, independent of h, such that

$$\sup_{(\mathbf{0},\mathbf{0})\neq(\boldsymbol{v}_h,\boldsymbol{\psi}_h)\in\boldsymbol{\mathcal{W}}_h} \frac{(\boldsymbol{q}_h, \boldsymbol{v}_h' - \boldsymbol{\psi}_h \times \boldsymbol{t})}{\|\boldsymbol{v}_h\|_1 + \|\boldsymbol{\psi}_h\|_1} \geqslant \beta_* \|\boldsymbol{q}_h\|_0 \quad \forall\, \boldsymbol{q}_h \in \boldsymbol{\mathcal{Q}}_h.$$

Property (i) has been proved in Arunakirinathar & Reddy (1993, Lemma 4.2) for $\widehat{\mathbb{E}}$ the identity matrix and $h > 0$ sufficiently small. The extension to $\widehat{\mathbb{E}}$ positive definite uniformly in s is quite straightforward. Property (ii) has been also proved in Arunakirinathar & Reddy (1993, Lemma 4.3) by means of a laborious constructive procedure, which is not fully detailed in this reference. In what follows, we provide an alternative, simpler proof, based on the arguments used by Chapelle (1997, Lemma 3, Step (ii)) for the discrete inf–sup condition arising from another discretization.

With this purpose, we will use the following lemma, which holds true as far as the rod is not a simple straight beam and whose proof can be found in Chapelle (1997, Lemma 1).

LEMMA 3.1 If $\boldsymbol{t}(s)$ is not a constant vector for all $s \in \mathrm{I}$, then there exists a linear mapping

$$\begin{aligned} \boldsymbol{\phi} : \mathbb{R}^3 &\longrightarrow \mathscr{C}^1(\mathrm{I}, \mathbb{R}^3), \\ \boldsymbol{x} &\longmapsto \boldsymbol{\phi}_{\boldsymbol{x}}, \end{aligned}$$

such that, for any $\boldsymbol{x} \in \mathbb{R}^3$,

$$\boldsymbol{\phi}_{\boldsymbol{x}}(0) = \boldsymbol{\phi}_{\boldsymbol{x}}(L) = \mathbf{0}, \tag{3.6}$$

$$\int_0^L \boldsymbol{\phi}_{\boldsymbol{x}}(s) \times \boldsymbol{t}(s)\mathrm{ds} = \boldsymbol{x}, \tag{3.7}$$

$$\|\boldsymbol{\phi}_{\boldsymbol{x}}\|_{\mathscr{C}^1(\mathrm{I},\mathbb{R}^3)} \leqslant C|\boldsymbol{x}|. \tag{3.8}$$

Note that the tangent vector $\boldsymbol{t}$ is constant throughout the length of the rod if and only if the rod is actually a straight beam. The finite-element scheme is perfectly well fitted in this case too (see the numerical results reported in Section 4.1 below). However, in such a case, the inf–sup condition in the following lemma must be proved by adapting the arguments used in Arnold (1981, p. 414), where a similar condition has been proved in a 2D simpler framework. For a curved rod, the following result holds.

LEMMA 3.2 For h small enough, there exists $\beta_* > 0$, independent of h, such that

$$\sup_{(\mathbf{0},\mathbf{0})\neq(\boldsymbol{v}_h,\boldsymbol{\psi}_h)\in\boldsymbol{\mathcal{W}}_h} \frac{(\boldsymbol{q}_h, \boldsymbol{v}_h' - \boldsymbol{\psi}_h \times \boldsymbol{t})}{\|\boldsymbol{v}_h\|_1 + \|\boldsymbol{\psi}_h\|_1} \geqslant \beta_* \left\|\boldsymbol{q}_h\right\|_0 \quad \forall\, \boldsymbol{q}_h \in \boldsymbol{\mathcal{Q}}_h.$$

Proof. Given $\boldsymbol{q}_h \in \boldsymbol{\mathcal{Q}}_h$, let $\boldsymbol{v} \in \mathrm{H}^1(\mathrm{I})^3$ be the solution of the following initial-value problem:

$$\begin{cases} \boldsymbol{v}' \equiv \dot{\boldsymbol{v}} + \Gamma^{\mathrm{t}}\boldsymbol{v} = \boldsymbol{q}_h, & \text{in I}, \\ \boldsymbol{v}(0) = \mathbf{0}. \end{cases}$$

Since $\boldsymbol{v}(0) = \mathbf{0}$, Poincaré inequality leads to $\|\boldsymbol{v}\|_0 \leqslant C\|\boldsymbol{v}'\|_0$. Hence,

$$\|\boldsymbol{v}\|_1 = (\|\boldsymbol{v}\|_0^2 + \|\dot{\boldsymbol{v}}\|_0^2)^{1/2} \leqslant C\|\boldsymbol{q}_h\|_0. \tag{3.9}$$

Let $\widehat{\boldsymbol{v}} := \widehat{v}_1\boldsymbol{t} + \widehat{v}_2\boldsymbol{n} + \widehat{v}_3\boldsymbol{b}$, with

$$\widehat{v}_i(s) := \int_0^s \Pi v_i'(\sigma)\mathrm{d}\sigma, \quad 0 \leqslant s \leqslant L,\ i = 1, 2, 3,$$

where v_i are the components of $\boldsymbol{v}$ in the Frenet basis and Π is the $\mathrm{L}^2(\mathrm{I})$-orthogonal projection onto

$$\mathscr{Q}_h := \{q \in \mathrm{L}^2(\mathrm{I}) : q|_{[s_{j-1},s_j]} \in \mathscr{P}_{r-1},\ j = 1, \ldots, n\}.$$

Clearly $\widehat{v}_i' = \Pi v_i'$ and $\widehat{v}_i(0) = 0$, so that, from Poincaré inequality, the boundedness of Π and (3.9),

$$\|\widehat{\boldsymbol{v}}\|_1 \leqslant C\left(\sum_{i=1}^3 \|\Pi v_i'\|_0^2\right)^{1/2} \leqslant C\left(\sum_{i=1}^3 \|v_i'\|_0^2\right)^{1/2} \leqslant C\|\boldsymbol{q}_h\|_0. \tag{3.10}$$

Now, for all points s_j of the partition $\mathscr{T}_h$, we have

$$\widehat{v}_i(s_j) - v_i(s_j) = \int_0^{s_j} [\Pi v_i'(\sigma) - v_i'(\sigma)]\mathrm{d}\sigma = 0,$$

because the characteristic function of the interval $[0, s_j]$ belongs to $\mathscr{Q}_h$. Therefore, from Cauchy–Schwarz inequality, we have, for all $s \in [s_j, s_{j+1}]$,

$$|\widehat{v}_i(s) - v_i(s)|^2 = \left|\int_{s_j}^s [\Pi v_i'(\sigma) - v_i'(\sigma)]\mathrm{d}\sigma\right|^2 \leqslant |s - s_j| \int_{s_j}^{s_{j+1}} |\Pi v_i'(\sigma) - v_i'(\sigma)|^2\mathrm{d}\sigma.$$

By integrating on $[s_j, s_{j+1}]$ and summing for $j = 0, \ldots, n-1$, we obtain

$$\|\widehat{v}_i - v_i\|_0^2 \leqslant \frac{h^2}{2}\|\Pi v_i' - v_i'\|_0^2 \leqslant h^2\|v_i'\|_0^2,$$

which together with (3.9) yield

$$\|\widehat{\boldsymbol{v}} - \boldsymbol{v}\|_0 \leqslant h\|\dot{\boldsymbol{v}}\|_0 \leqslant Ch\|\boldsymbol{q}_h\|_0. \tag{3.11}$$

On the other hand, since $\widehat{v}_i' = \Pi v_i'$ and the components of $\boldsymbol{q}_h$ belong to $\mathscr{Q}_h$, according to the definition (2.1) of $\dot{\boldsymbol{v}}$ and $\hat{\boldsymbol{v}}$, we have

$$(\boldsymbol{q}_h, \hat{\boldsymbol{v}}) = (\boldsymbol{q}_h, \dot{\boldsymbol{v}}) = (\boldsymbol{q}_h, \boldsymbol{v}') - (\boldsymbol{q}_h, \Gamma^{\mathrm{t}}\boldsymbol{v}),$$

which together with the definition of $\boldsymbol{v}$ leads to

$$(\boldsymbol{q}_h, \widehat{\boldsymbol{v}}') = (\boldsymbol{q}_h, \hat{\boldsymbol{v}}) + (\boldsymbol{q}_h, \Gamma^{\mathrm{t}}\widehat{\boldsymbol{v}}) = (\boldsymbol{q}_h, \boldsymbol{v}') + (\boldsymbol{q}_h, \Gamma^{\mathrm{t}}(\widehat{\boldsymbol{v}} - \boldsymbol{v})) = \|\boldsymbol{q}_h\|_0^2 + (\boldsymbol{q}_h, \Gamma^{\mathrm{t}}(\widehat{\boldsymbol{v}} - \boldsymbol{v})).$$

Thus, from (3.11), we obtain

$$(\boldsymbol{q}_h, \widehat{\boldsymbol{v}}') \geqslant (1 - Ch)\|\boldsymbol{q}_h\|_0^2. \tag{3.12}$$

According to the definition, $\widehat{v}_i$ are piecewise $\mathscr{P}_r$ continuous functions vanishing at $s = 0$. However, in general, $\widehat{\boldsymbol{v}}(L) \neq \boldsymbol{0}$, so that $\widehat{\boldsymbol{v}} \notin \boldsymbol{\mathscr{V}}_h$. Because of this, we resort to Lemma 3.1.

Let $\boldsymbol{x} := -\widehat{\boldsymbol{v}}(L)$ and $\boldsymbol{\phi}_{\boldsymbol{x}}$ be as in Lemma 3.1. From (3.8) and (3.10), we have

$$\|\boldsymbol{\phi}_{\boldsymbol{x}}\|_1 \leqslant C\|\boldsymbol{\phi}_{\boldsymbol{x}}\|_{\mathscr{C}^1(\mathrm{I},\mathbb{R}^3)} \leqslant C|\boldsymbol{x}| \leqslant C\|\widehat{\boldsymbol{v}}\|_1 \leqslant C\|\boldsymbol{q}_h\|_0.$$

Let

$$\boldsymbol{w}(s) := \int_0^s \boldsymbol{\phi}_{\boldsymbol{x}}(\sigma) \times \boldsymbol{t}(\sigma)\mathrm{d}\sigma, \quad 0 \leqslant s \leqslant L.$$

Clearly, $\boldsymbol{w}(0) = \boldsymbol{0}$ and $\boldsymbol{w}' = \boldsymbol{\phi}_{\boldsymbol{x}} \times \boldsymbol{t}$. Hence, from Poincaré inequality,

$$\|\boldsymbol{w}\|_1 \leqslant C\|\boldsymbol{w}'\|_0 \leqslant C\|\boldsymbol{\phi}_{\boldsymbol{x}}\|_0 \leqslant C\|\boldsymbol{q}_h\|_0.$$

Let $\boldsymbol{\phi}_{\boldsymbol{x}}^{\mathrm{I}}$ and $\boldsymbol{w}^{\mathrm{I}}$ be the vector fields whose components in the Frenet basis are the Lagrange interpolants of degree r of the respective components of $\boldsymbol{\phi}_{\boldsymbol{x}}$ and $\boldsymbol{w}$ in the same basis. Standard properties of the 1D Lagrange interpolant yield

$$\|\boldsymbol{\phi}_{\boldsymbol{x}}^{\mathrm{I}}\|_1 \leqslant C\|\boldsymbol{\phi}_{\boldsymbol{x}}\|_1 \leqslant C\|\boldsymbol{q}_h\|_0 \quad \text{and} \quad \|\boldsymbol{w}^{\mathrm{I}}\|_1 \leqslant C\|\boldsymbol{w}\|_1 \leqslant C\|\boldsymbol{q}_h\|_0, \tag{3.13}$$

as well as

$$\|\boldsymbol{\phi}_{\boldsymbol{x}} - \boldsymbol{\phi}_{\boldsymbol{x}}^{\mathrm{I}}\|_0 \leqslant Ch\|\dot{\boldsymbol{\phi}}_{\boldsymbol{x}}\|_0 \leqslant Ch\|\boldsymbol{q}_h\|_0,$$

$$\|(\boldsymbol{w}^{\mathrm{I}} - \boldsymbol{w})'\|_0 \leqslant \|(\boldsymbol{w}^{\mathrm{I}} - \boldsymbol{w})^{\cdot}\|_0 + \|\Gamma^{\mathrm{t}}(\boldsymbol{w}^{\mathrm{I}} - \boldsymbol{w})\|_0 \leqslant Ch(\|\ddot{\boldsymbol{w}}\|_0 + \|\dot{\boldsymbol{w}}\|_0) \leqslant Ch\|\boldsymbol{q}_h\|_0.$$

The latter holds because $\ddot{\boldsymbol{w}} = (\boldsymbol{w}' - \Gamma^{\mathrm{t}}\boldsymbol{w})^{\cdot} = (\boldsymbol{\phi}_{\boldsymbol{x}} \times \boldsymbol{t})^{\cdot} - (\Gamma^{\mathrm{t}}\boldsymbol{w})^{\cdot}$ and, consequently, $\|\ddot{\boldsymbol{w}}\|_0 \leqslant C(\|\boldsymbol{\phi}_{\boldsymbol{x}}\|_1 + \|\boldsymbol{w}\|_1)$. Therefore,

$$|(\boldsymbol{q}_h, (\boldsymbol{w}^{\mathrm{I}})' - \boldsymbol{\phi}_{\boldsymbol{x}}^{\mathrm{I}} \times \boldsymbol{t})| = |(\boldsymbol{q}_h, (\boldsymbol{w}^{\mathrm{I}} - \boldsymbol{w})') + (\boldsymbol{q}_h, (\boldsymbol{\phi}_{\boldsymbol{x}} - \boldsymbol{\phi}_{\boldsymbol{x}}^{\mathrm{I}}) \times \boldsymbol{t})| \leqslant Ch\|\boldsymbol{q}_h\|_0^2. \tag{3.14}$$

Finally, let $\boldsymbol{v}_h := \widehat{\boldsymbol{v}} + \boldsymbol{w}^{\mathrm{I}}$ and $\boldsymbol{\psi}_h := \boldsymbol{\phi}_{\boldsymbol{x}}^{\mathrm{I}}$. Because of (3.6) and (3.7), both belong to $\mathscr{W}_h$. From (3.10) and (3.13), we have

$$\|\boldsymbol{v}_h\|_1 + \|\boldsymbol{\psi}_h\|_1 \leqslant C\|\boldsymbol{q}_h\|_0,$$

whereas from (3.12) and (3.14),

$$(\boldsymbol{q}_h, \boldsymbol{v}_h' - \boldsymbol{\psi}_h \times \boldsymbol{t}) \geqslant (1 - Ch)\|\boldsymbol{q}_h\|_0^2. \tag{3.15}$$

The last two inequalities allow us to conclude the lemma. □

REMARK 3.3 The proof of the inf–sup condition in the previous lemma needs h to be sufficiently small, in order to have $1 - Ch > 0$ in (3.15). A similar condition is assumed in the proofs of Arunakirinathar & Reddy (1993, Lemma 4.3) and Chapelle (1997, Lemma 3). The same assumption is made in Arunakirinathar & Reddy (1993, Lemma 4.2) as well, to prove the ellipticity in the discrete kernel property (3.5). Because of this, h will be assumed to be small enough in all the following theorems. However, this hypothesis seems to be a technicality. In fact, we have not observed a need for this assumption in any of the numerical experiments reported in Section 4 below.

Now we are in a position to prove that T_h is well defined and converges to T as $h \to 0$.

THEOREM 3.4 For sufficiently small $h > 0$, problem (3.3)–(3.4) has a unique solution $(\boldsymbol{u}_h, \boldsymbol{\theta}_h, \boldsymbol{\gamma}_h) \in \boldsymbol{\mathcal{W}}_h \times \boldsymbol{\mathcal{Q}}_h$. This solution satisfies

$$\|\boldsymbol{u}_h\|_1 + \|\boldsymbol{\theta}_h\|_1 + \|\boldsymbol{\gamma}_h\|_0 \leqslant C(\|\boldsymbol{f}\|_0 + d^2\|\boldsymbol{\phi}\|_0), \tag{3.16}$$

where $C > 0$ is independent of h and d.

Let $(\boldsymbol{u}, \boldsymbol{\theta}, \boldsymbol{\gamma}) \in \boldsymbol{\mathcal{W}} \times \boldsymbol{\mathcal{Q}}$ be the solution of problem (2.6)–(2.7). If $\boldsymbol{f}, \boldsymbol{\phi} \in H^{k-1}(\mathrm{I})^3$, $1 \leqslant k \leqslant r$, then

$$\|\boldsymbol{u} - \boldsymbol{u}_h\|_1 + \|\boldsymbol{\theta} - \boldsymbol{\theta}_h\|_1 + \|\boldsymbol{\gamma} - \boldsymbol{\gamma}_h\|_0 \leqslant Ch^k(\|\boldsymbol{f}\|_{k-1} + d^2\|\boldsymbol{\phi}\|_{k-1}), \tag{3.17}$$

$$\|\boldsymbol{u} - \boldsymbol{u}_h\|_0 + \|\boldsymbol{\theta} - \boldsymbol{\theta}_h\|_0 \leqslant Ch^{k+1}(\|\boldsymbol{f}\|_{k-1} + d^2\|\boldsymbol{\phi}\|_{k-1}), \tag{3.18}$$

with $C > 0$ independent of h and d.

Proof. By virtue of (3.5) and Lemma 3.2, the well-posedness of problem (3.3)–(3.4) as well as the error estimate (3.17) are consequences of Proposition II.2.11 from Brezzi & Fortin (1991). On the other hand, (3.18) is obtained by adapting to our case the duality argument used to prove Theorem 2 from Chapelle (1997). □

By adding (3.3) and (3.4), from the symmetry of the resulting bilinear forms, it is immediate to show that T_h is self-adjoint with respect to the weighted $\mathrm{L}^2(\mathrm{I})^3 \times \mathrm{L}^2(\mathrm{I})^3$ inner product in the right-hand side of (3.3). Therefore, apart from $\mu_h = 0$, the spectrum of T_h consists of a finite number of finite-multiplicity real eigenvalues with ascent one.

Once more, the spectrum of the operator T_h is related with the eigenvalues of the spectral problem (3.1)–(3.2): λ_h is a nonzero eigenvalue of this problem if and only if $\mu_h := 1/\lambda_h$ is a nonzero eigenvalue of T_h, with the same multiplicity and corresponding eigenfunctions. These eigenvalues are strictly positive. Indeed, by taking $\boldsymbol{v}_h = \boldsymbol{u}_h$, $\boldsymbol{\psi}_h = \boldsymbol{\theta}_h$ and $\boldsymbol{q}_h = \boldsymbol{\gamma}_h$ in problem (3.1)–(3.2), by subtracting the second equation from the first one, we have

$$\lambda_h = \frac{(\widehat{\mathbb{E}}\boldsymbol{\theta}_h', \boldsymbol{\theta}_h') + d^2(\widehat{\mathbb{D}}^{-1}\boldsymbol{\gamma}_h, \boldsymbol{\gamma}_h)}{(\widehat{A}\boldsymbol{u}_h, \boldsymbol{u}_h) + d^2(\widehat{\mathbb{J}}\boldsymbol{\theta}_h, \boldsymbol{\theta}_h)} \geqslant 0.$$

Moreover, the eigenvalues cannot vanish. In fact, according to the expression above, since $\widehat{\mathbb{E}}$ and $\widehat{\mathbb{D}}$ are positive definite (see Remark 2.3), $\lambda_h = 0$ would imply $\boldsymbol{\gamma}_h = 0$. Then, (3.2) would imply that $(\boldsymbol{u}_h, \boldsymbol{\theta}_h) \in \boldsymbol{\mathcal{W}}_{0h}$ and, hence, $\boldsymbol{u}_h$ and $\boldsymbol{\theta}_h$ would vanish too because of (3.5).

Our aim is to use the spectral theory for compact operators (see Babuška & Osborn, 1991, for instance) to prove convergence of the eigenvalues and eigenfunctions of T_h towards those of T. However, some further considerations will be needed to show that the error estimates do not deteriorate as d becomes small. With this purpose, we will use the following result:

$$\|(T - T_h)(\boldsymbol{f}, \boldsymbol{\phi})\|_1 \leqslant Ch(\|\boldsymbol{f}\|_0 + d^2\|\boldsymbol{\phi}\|_0), \tag{3.19}$$

which follows from (3.17) with $k = 1$. As a consequence of this estimate, T_h converges in norm to T as h goes to zero. Hence, standard results of spectral approximation (see for instance Kato, 1995) show that if μ is an eigenvalue of T with multiplicity m, then exactly m eigenvalues $\mu_h^{(1)}, \ldots, \mu_h^{(m)}$ of T_h (repeated according to their respective multiplicities) converge to μ.

The estimate above can be improved when the source term is an eigenfunction $(\boldsymbol{u}, \boldsymbol{\theta})$ of T. Indeed, in such a case, the same arguments used to prove (2.11) allow us to show that, for all $k \geqslant 2$ and d sufficiently small, we have

$$\|\boldsymbol{u}\|_k + \|\boldsymbol{\theta}\|_k + \|\boldsymbol{\gamma}\|_{k-1} \leqslant C(\|\boldsymbol{u}\|_0 + d^2\|\boldsymbol{\theta}\|_0), \tag{3.20}$$

with C depending on k and on the eigenvalue of T associated with $(\boldsymbol{u}, \boldsymbol{\theta})$. Note that, in principle, the constant C should depend also on d, because the eigenvalue does so. However, according to Lemma 2.6, for d sufficiently small we can choose C independent of d. Hence, from (3.17)–(3.18) with $k = r$, we obtain

$$\|(T - T_h)(\boldsymbol{u}, \boldsymbol{\theta})\|_1 \leqslant Ch^r \|(\boldsymbol{u}, \boldsymbol{\theta})\|_1, \tag{3.21}$$

$$\|(T - T_h)(\boldsymbol{u}, \boldsymbol{\theta})\|_0 \leqslant Ch^{r+1} \|(\boldsymbol{u}, \boldsymbol{\theta})\|_0. \tag{3.22}$$

Here and hereafter, $\|\cdot\|_0$ denotes the standard product norm in $\mathrm{L}^2(\mathrm{I})^3 \times \mathrm{L}^2(\mathrm{I})^3$.

We remind zaders of the definition of the 'gap' or symmetric distance $\widehat{\delta}_k$ between closed subspaces $\mathscr{Y}$ and $\mathscr{Z}$ of $\mathscr{W}$ in norm $\|\cdot\|_k$, $k = 0, 1$:

$$\widehat{\delta}_k(\mathscr{Y}, \mathscr{Z}) := \max\{\delta_k(\mathscr{Y}, \mathscr{Z}), \delta_k(\mathscr{Z}, \mathscr{Y})\},$$

with

$$\delta_k(\mathscr{Y}, \mathscr{Z}) := \sup_{\substack{(\boldsymbol{v}, \boldsymbol{\psi}) \in \mathscr{Y} \\ \|(\boldsymbol{v}, \boldsymbol{\psi})\|_k = 1}} \left[\inf_{(\widehat{\boldsymbol{v}}, \widehat{\boldsymbol{\psi}}) \in \mathscr{Z}} \|(\boldsymbol{v} - \widehat{\boldsymbol{v}}, \boldsymbol{\psi} - \widehat{\boldsymbol{\psi}})\|_k \right].$$

For the sake of simplicity, we state our results for eigenvalues of T converging to a simple eigenvalue of T_0 as $d \to 0$ (at the end of this section, we will discuss this assumption). The following theorem yields d-independent error estimates for the approximate eigenvalues and eigenfunctions.

THEOREM 3.5 Let μ be an eigenvalue of T converging to a simple eigenvalue μ_0 of T_0 as d tends to zero. Let μ_h be the eigenvalue of T_h that converges to μ as h tends to zero. Let $\mathscr{E}$ and $\mathscr{E}_h$ be the corresponding eigenspaces. Then, for d and h small enough

$$\widehat{\delta}_1(\mathscr{E}, \mathscr{E}_h) \leqslant Ch^r, \tag{3.23}$$

$$\widehat{\delta}_0(\mathscr{E}, \mathscr{E}_h) \leqslant Ch^{r+1}, \tag{3.24}$$

$$|\mu - \mu_h| \leqslant Ch^r, \tag{3.25}$$

with $C > 0$ independent of d and h.

Proof. The estimates are direct consequences of (3.21)–(3.22) and Theorems 7.1 and 7.2 from Babuška & Osborn (1991), in all cases with C depending on the constants in (3.21)–(3.22) and on the inverse of the distance from μ to the rest of the spectrum of T. Now using Lemma 2.6, we see that for d small enough, this distance is bounded below in terms of the distance from μ_0 to the rest of the spectrum of T_0, which obviously depends neither on d nor on h. This allows us to conclude the proof. □

This theorem yields optimal-order error estimates for the approximate eigenfunctions in norms $\|\cdot\|_1$ and $\|\cdot\|_0$. In fact, the theorem implies that the eigenfunctions $(\boldsymbol{u}, \boldsymbol{\theta})$ of T and $(\boldsymbol{u}_h, \boldsymbol{\theta}_h)$ of T_h, corresponding to the eigenvalues μ and μ_h, respectively, can be chosen normalized in $\|\cdot\|_k$, $k = 0, 1$, and so that

$$\|\boldsymbol{u} - \boldsymbol{u}_h\|_1 + \|\boldsymbol{\theta} - \boldsymbol{\theta}_h\|_1 \leqslant Ch^r \qquad (k = 1), \tag{3.26}$$

$$\|\boldsymbol{u} - \boldsymbol{u}_h\|_0 + \|\boldsymbol{\theta} - \boldsymbol{\theta}_h\|_0 \leqslant Ch^{r+1} \quad (k = 0), \tag{3.27}$$

which are the optimal orders for the finite elements used. Instead, the order of the error estimate (3.25) is not optimal. To improve this result, we will have to study first the convergence of the shear stresses of the vibration modes.

LEMMA 3.6 Let μ and μ_h be as in Theorem 3.5. Let $(\boldsymbol{u}, \boldsymbol{\theta}, \boldsymbol{\gamma})$ be a solution of problem (2.4)–(2.5) with $\lambda = \frac{1}{\mu}$, and $(\boldsymbol{u}_h, \boldsymbol{\theta}_h, \boldsymbol{\gamma}_h)$ a solution of problem (3.1)–(3.2) with $\lambda_h = \frac{1}{\mu_h}$, such that $\|(\boldsymbol{u}, \boldsymbol{\theta})\|_1 = \|(\boldsymbol{u}_h, \boldsymbol{\theta}_h)\|_1^1 = 1$ and (3.26) holds true. Then, for d and h small enough

$$\|\boldsymbol{\gamma} - \boldsymbol{\gamma}_h\|_0 \leqslant Ch^r,$$

with $C > 0$ independent of d and h.

Proof. From (3.1) and (2.4), we have, for all $(\boldsymbol{v}_h, \boldsymbol{\psi}_h) \in \boldsymbol{\mathcal{W}}_h$,

$$\begin{aligned}(\boldsymbol{\gamma} - \boldsymbol{\gamma}_h, \boldsymbol{v}_h' - \boldsymbol{\psi}_h \times \boldsymbol{t}) &= \lambda[(\widehat{A}(\boldsymbol{u} - \boldsymbol{u}_h), \boldsymbol{v}_h) + d^2(\widehat{\mathbb{J}}(\boldsymbol{\theta} - \boldsymbol{\theta}_h), \boldsymbol{\psi}_h)] \\ &\quad + (\lambda - \lambda_h)[(\widehat{A}\boldsymbol{u}_h, \boldsymbol{v}_h) + d^2(\widehat{\mathbb{J}}\boldsymbol{\theta}_h, \boldsymbol{\psi}_h)] - (\widehat{\mathbb{E}}(\boldsymbol{\theta}' - \boldsymbol{\theta}_h'), \boldsymbol{\psi}_h') \\ &\leqslant Ch^r(\|\boldsymbol{v}_h\|_1 + \|\boldsymbol{\psi}_h\|_1),\end{aligned}$$

where we have used (3.25) and (3.26) for the last inequality. Note that the constant C depends on the eigenvalue λ, but not on d or h, for d small enough (Lemma 2.6). Using this estimate, we have, for all $\widehat{\boldsymbol{\gamma}} \in \boldsymbol{\mathcal{Q}}_h$ and for all $(\boldsymbol{v}_h, \boldsymbol{\psi}_h) \in \boldsymbol{\mathcal{W}}_h$,

$$(\widehat{\boldsymbol{\gamma}} - \boldsymbol{\gamma}_h, \boldsymbol{v}_h' - \boldsymbol{\psi}_h \times \boldsymbol{t}) \leqslant (\widehat{\boldsymbol{\gamma}} - \boldsymbol{\gamma}, \boldsymbol{v}_h' - \boldsymbol{\psi}_h \times \boldsymbol{t}) + Ch^r(\|\boldsymbol{v}_h\|_1 + \|\boldsymbol{\psi}_h\|_1).$$

Therefore, from Lemma 3.2 we have, for all $\widehat{\boldsymbol{\gamma}} \in \boldsymbol{\mathcal{Q}}_h$,

$$\beta_*\|\widehat{\boldsymbol{\gamma}} - \boldsymbol{\gamma}_h\|_0 \leqslant \sup_{(\boldsymbol{0},\boldsymbol{0}) \neq (\boldsymbol{v}_h, \boldsymbol{\psi}_h) \in \boldsymbol{\mathcal{W}}_h} \frac{(\widehat{\boldsymbol{\gamma}} - \boldsymbol{\gamma}_h, \boldsymbol{v}_h' - \boldsymbol{\psi}_h \times \boldsymbol{t})}{\|\boldsymbol{v}_h\|_1 + \|\boldsymbol{\psi}_h\|_1} \leqslant C(\|\widehat{\boldsymbol{\gamma}} - \boldsymbol{\gamma}\|_0 + h^r).$$

Hence, if we choose $\widehat{\boldsymbol{\gamma}}$ as the $\mathrm{L}^2(\mathrm{I})^3$-projection of $\boldsymbol{\gamma}$ onto $\boldsymbol{\mathcal{Q}}_h$, the theorem follows from the triangular inequality, standard error estimates of the projection and (3.20). □

Now we are in a position to prove an optimal order of convergence for the approximate eigenvalues by adapting to our problem a standard argument for variationally posed eigenvalue problems (see Babuška & Osborn, 1991, Lemma 9.1, for instance).

THEOREM 3.7 Let $\lambda = \frac{1}{\mu}$ and $\lambda_h = \frac{1}{\mu_h}$, with μ and μ_h as in Theorem 3.5. Then, for d and h small enough

$$|\lambda - \lambda_h| \leqslant Ch^{2r}, \tag{3.28}$$

with $C > 0$ independent of d and h.

Proof. Let $\mathscr{A}_d$ and $\mathscr{B}_d$ denote the symmetric and continuous bilinear forms defined in $\boldsymbol{\mathcal{W}} \times \boldsymbol{\mathcal{Q}}$ as

$$\mathscr{A}_d((\boldsymbol{u}, \boldsymbol{\theta}, \boldsymbol{\gamma}), (\boldsymbol{v}, \boldsymbol{\psi}, \boldsymbol{q})) := (\widehat{\mathbb{E}}\boldsymbol{\theta}', \boldsymbol{\psi}') + (\boldsymbol{\gamma}, \boldsymbol{v}' - \boldsymbol{\psi} \times \boldsymbol{t}) + (\boldsymbol{u}' - \boldsymbol{\theta} \times \boldsymbol{t}, \boldsymbol{q}) - d^2(\widehat{\mathbb{D}}^{-1}\boldsymbol{\gamma}, \boldsymbol{q}),$$

$$\mathscr{B}_d((\boldsymbol{u}, \boldsymbol{\theta}, \boldsymbol{\gamma}), (\boldsymbol{v}, \boldsymbol{\psi}, \boldsymbol{q})) := (\widehat{A}\boldsymbol{u}, \boldsymbol{v}) + d^2(\widehat{\mathbb{J}}\boldsymbol{\theta}, \boldsymbol{\psi}).$$

Using this notation, problems (2.4)–(2.5) and (3.1)–(3.2) are, respectively, written as follows:

$$\mathscr{A}_d((\boldsymbol{u}, \boldsymbol{\theta}, \boldsymbol{\gamma}), (\boldsymbol{v}, \boldsymbol{\psi}, \boldsymbol{q})) = \lambda\mathscr{B}_d((\boldsymbol{u}, \boldsymbol{\theta}, \boldsymbol{\gamma}), (\boldsymbol{v}, \boldsymbol{\psi}, \boldsymbol{q})) \quad \forall (\boldsymbol{v}, \boldsymbol{\psi}) \in \boldsymbol{\mathcal{W}} \ \forall \boldsymbol{q} \in \boldsymbol{\mathcal{Q}};$$

$$\mathscr{A}_d((\boldsymbol{u}_h, \boldsymbol{\theta}_h, \boldsymbol{\gamma}_h), (\boldsymbol{v}_h, \boldsymbol{\psi}_h, \boldsymbol{q}_h)) = \lambda_h\mathscr{B}_d((\boldsymbol{u}_h, \boldsymbol{\theta}_h, \boldsymbol{\gamma}_h), (\boldsymbol{v}_h, \boldsymbol{\psi}_h, \boldsymbol{q}_h)) \quad \forall (\boldsymbol{v}_h, \boldsymbol{\psi}_h) \in \boldsymbol{\mathcal{W}}_h \ \forall \boldsymbol{q}_h \in \boldsymbol{\mathcal{Q}}_h.$$

Consider eigenfunctions satisfying $\|(\boldsymbol{u}, \boldsymbol{\theta})\|_1 = \|(\boldsymbol{u}_h, \boldsymbol{\theta}_h)\|_1 = 1$ and (3.26).

From the symmetry of the bilinear forms, straightforward computations lead to

$$\begin{aligned}(\lambda-\lambda_h)&\mathscr{B}_d((\boldsymbol{u}_h,\boldsymbol{\theta}_h,\boldsymbol{\gamma}_h),(\boldsymbol{u}_h,\boldsymbol{\theta}_h,\boldsymbol{\gamma}_h))\\&=\lambda\mathscr{B}_d((\boldsymbol{u}-\boldsymbol{u}_h,\boldsymbol{\theta}-\boldsymbol{\theta}_h,\boldsymbol{\gamma}-\boldsymbol{\gamma}_h),(\boldsymbol{u}-\boldsymbol{u}_h,\boldsymbol{\theta}-\boldsymbol{\theta}_h,\boldsymbol{\gamma}-\boldsymbol{\gamma}_h))\\&\quad-\mathscr{A}_d((\boldsymbol{u}-\boldsymbol{u}_h,\boldsymbol{\theta}-\boldsymbol{\theta}_h,\boldsymbol{\gamma}-\boldsymbol{\gamma}_h),(\boldsymbol{u}-\boldsymbol{u}_h,\boldsymbol{\theta}-\boldsymbol{\theta}_h,\boldsymbol{\gamma}-\boldsymbol{\gamma}_h)).\end{aligned}$$

By using (3.16) with $\boldsymbol{f}=\lambda_h\boldsymbol{u}_h$ and $\boldsymbol{\phi}=\lambda_h\boldsymbol{\theta}_h$, we have

$$\mathscr{B}_d((\boldsymbol{u}_h,\boldsymbol{\theta}_h,\boldsymbol{\gamma}_h),(\boldsymbol{u}_h,\boldsymbol{\theta}_h,\boldsymbol{\gamma}_h))\geqslant C(\|\boldsymbol{u}_h\|_0^2+d^2\|\boldsymbol{\theta}_h\|_0^2)\geqslant\frac{C}{\lambda_h^2}(\|\boldsymbol{u}_h\|_1^2+\|\boldsymbol{\theta}_h\|_1^2)=\frac{C}{\lambda_h^2}.$$

Hence, from the continuity of the bilinear forms, we obtain

$$|\lambda-\lambda_h|\leqslant C(\|\boldsymbol{u}-\boldsymbol{u}_h\|_1+\|\boldsymbol{\theta}-\boldsymbol{\theta}_h\|_1+\|\boldsymbol{\gamma}-\boldsymbol{\gamma}_h\|_0)^2,$$

with C depending on λ and λ_h, but neither on d nor on h, for d and h sufficiently small (Lemma 2.6 and (3.25)). Thus, (3.26) and Lemma 3.6 allow us to conclude the proof. □

The last two theorems have been settled for eigenvalues of T converging to simple eigenvalues of T_0 as $d\to 0$. A multiple eigenvalue of T_0 usually arises because of symmetries in the geometry of the rod; in such a case, the eigenvalue of T converging to it has the same multiplicity. The proofs of these theorems extend trivially to cover this case.

Instead, if T_0 had a multiple eigenvalue not due to symmetry reasons, it could split into different eigenvalues of T. In this case, the proofs of the theorems above do not provide estimates independent of the thickness. In fact, the constants therein might in principle blow up as the distance between the eigenvalues becomes smaller.

However, by combining Lemma 2.5 and (3.19) we have

$$\|(T_h-T_0)(\boldsymbol{f},\boldsymbol{\phi})\|_1\leqslant C(d+h)(\|\boldsymbol{f}\|_0+d^2\|\boldsymbol{\phi}\|_0)\quad\forall\boldsymbol{f},\boldsymbol{\phi}\in\mathrm{L}^2(\mathrm{I})^3.$$

This estimate can be used to prove spectral convergence as d and h both converge to zero. In fact, if μ_0 is an eigenvalue of T_0 with multiplicity m, then there exist exactly m eigenvalues $\mu_h^{(1)},\dots,\mu_h^{(m)}$ of T_h (repeated according to their respective multiplicities) converging to μ_0 as d and h go to zero (see again Kato, 1995). Let $\mathscr{E}_0$ be the eigenspace of T_0 corresponding to μ_0 and let $\mathscr{E}_h$ be the direct sum of the eigenspaces of T_h corresponding to $\mu_h^{(1)},\dots,\mu_h^{(m)}$. Then, by proceeding as in the proof of Theorem 3.5, we obtain

$$\begin{aligned}\widehat{\delta}_1(\mathscr{E}_0,\mathscr{E}_h)&\leqslant C(d+h^r),\\\widehat{\delta}_0\left(\mathscr{E}_0,\mathscr{E}_h\right)&\leqslant C(d+h^{r+1}).\end{aligned}$$

Moreover, the arguments in the proofs of Lemma 3.6 and Theorem 3.7 can be easily adapted to take into account some additional $\mathscr{O}(d^2)$ terms, leading to similar results. In particular, the following estimate holds true for $\lambda_0=\frac{1}{\mu_0}$ and $\lambda_h^{(j)}=\frac{1}{\mu_h^{(j)}}$:

$$|\lambda_0-\lambda_h^{(j)}|\leqslant C(d^2+h^{2r}),\quad j=1,\dots,m.$$

4. Numerical results

We report in this section the results of some numerical tests computed with a MATLAB code implementing the finite-element method described above. We have used the lowest possible order: $r = 1$; namely, piecewise linear continuous elements for the displacements $\boldsymbol{u}_h$ and the rotations $\boldsymbol{\theta}_h$ and piecewise constant discontinuous elements for the shear stresses $\boldsymbol{\gamma}_h$.

We have computed the vibration modes with lowest frequencies $\omega^h := \sqrt{\lambda_h}$ for straight, circular and helical rods, with different sections, thickness and boundary conditions. To help identify the different modes, we report 2D plots of the computed components of displacements and rotations in the Frenet basis, as well as the 3D deformed rods. For the latter, we have used MODULEF to create an auxiliary hexahedral mesh of the actual 3D rod and the displacements at each node of this auxiliary mesh have been computed from $\boldsymbol{u}_h$ and $\boldsymbol{\theta}_h$ as described in Remark 2.2. The resulting deformed rods have also been plotted with MODULEF.

In all cases, we have computed the lowest vibration frequencies $\omega_1^h < \omega_2^h < \omega_3^h < \cdots$ by using uniform meshes of N elements, with different values of N. Also, in all cases we have used the following physical parameters, which correspond to steel:

- elastic moduli: $E = 2.1 \times 10^6\,\mathrm{kgf/cm^2}$ ($1\,\mathrm{kgf} = 980\,\mathrm{kg\,cm/s^2}$);
- Poisson coefficient: $\nu = 0.3 \quad (G = E/[2(1+\nu)])$;
- density: $\rho = 7.85 \times 10^{-3}\,\mathrm{kg/cm^3}$;
- correction factors: $k_1 = k_2 = 1$.

4.1 *Test 1: a straight beam*

The aim of this first test is to validate the computer code by solving a problem with a known analytical solution. With this purpose, we have computed the vibration modes of a beam (i.e. a straight rod, which corresponds to $\kappa = \tau = 0$). We have taken the beam clamped at both ends, with a total length $L = 120\,\mathrm{cm}$, and a square cross-section of side length $b = 20\,\mathrm{cm}$. Therefore, the nondimensional thickness parameter is in this case $d = 0.068$. Figure 2 shows the undeformed beam.

To estimate the order of convergence of the method, we have compared the computed vibration frequencies with the closed form solution given in Huang (1961) for the flexural modes. The analytical solutions of the torsional and axial modes have been obtained by means of straightforward algebraic manipulations.

Table 1 shows the lowest vibration frequencies computed on successively refined meshes. It also includes the computed orders of convergence and the corresponding exact vibration frequencies ω_{ex}. Finally 'd' and 's' point out if the vibration frequencies correspond to double or simple eigenvalues, respectively.

Figures 3–5 show the lowest-frequency vibration modes. Those corresponding to the frequencies ω_1 and ω_3 are flexural modes, whereas that corresponding to the frequency ω_2 is torsional. For each mode, the figures show the components in the Frenet basis of the displacements, $\boldsymbol{u}$, and the rotations, $\boldsymbol{\theta}$, as well as the deformed beam.

As indicated in Table 1, ω_1 and ω_3 correspond to double-multiplicity eigenvalues. The planar vibration modes shown in Figs 3 and 5 only involve deformations in the plane spanned by $\boldsymbol{t}$ and $\boldsymbol{n}$. The eigenspaces of each of these eigenvalues also contain other planar vibration modes involving deformations in the plane spanned by $\boldsymbol{t}$ and $\boldsymbol{b}$. They are not shown because they are exactly the same as those in Figs 3 and 5, rotated by 90° with respect to the axis $\boldsymbol{t}$.

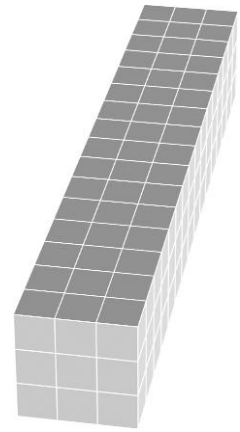

FIG. 2. Undeformed straight beam.

TABLE 1 *Angular vibration frequencies of a straight beam*

Mode	$N = 16$	$N = 32$	$N = 64$	$N = 128$	Order	ω_{ex}	d/s
ω_1^h	4034.05	4005.16	3997.99	3996.20	2.00	3995.61	d
ω_2^h	8326.58	8316.57	8314.06	8313.44	2.00	8313.22	s
ω_3^h	9818.49	9656.86	9617.04	9607.11	2.01	9603.80	d
ω_4^h	13426.22	13410.07	13406.03	13405.03	2.00	13404.69	s
ω_5^h	17101.68	16639.02	16525.57	16497.37	2.01	16487.94	d
ω_6^h	16733.53	16653.17	16633.13	16628.13	2.00	16626.47	s

4.2 *Test 2: a helical rod*

The aim of this test is to apply the finite-element method to a more general curved nonplanar rod with nonvanishing curvature and torsion. We have considered a helix with eight turns, clamped at both ends. The equation of the helix centroids line parametrized by its arc length is as follows:

$$\boldsymbol{r}(s) = \left(A\cos\frac{s}{n}, A\sin\frac{s}{n}, C\frac{s}{n}\right), \quad \text{with } n = \sqrt{A^2 + C^2}, \tag{4.1}$$

the curvature is $\kappa = A/n^2$, the torsion $\tau = C/n^2$ and the length of the eight-turns helix is $L = 8 \times 2\pi n$. We have taken $A = 100\,\text{cm}$, $C = 25/\pi$ cm and a square of side length $b = 20$ cm as the cross-section of the rod. Thus, the thickness parameter is in this case $d = 0.0016$. Figure 6 shows the undeformed helix.

Since no analytical solution is available for this rod, we have estimated the order of convergence by means of a least squares fitting of the model

$$\omega_j^h \approx \omega_{ex} + Ch^t.$$

Table 2 shows the lowest vibration frequencies computed on successively refined meshes. It also includes the computed orders of convergence t and the 'exact' vibration frequencies ω_{ex}, obtained with this fitting.

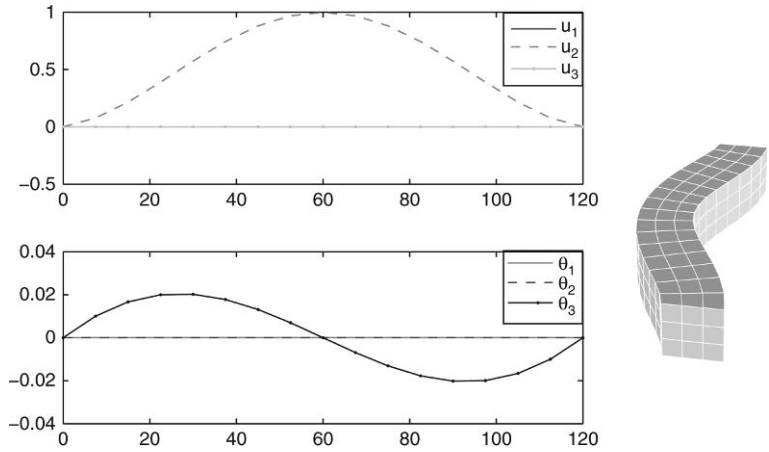

FIG. 3. Straight beam. Vibration mode of frequency ω_1. Displacements and rotations (left). Deformed beam (right).

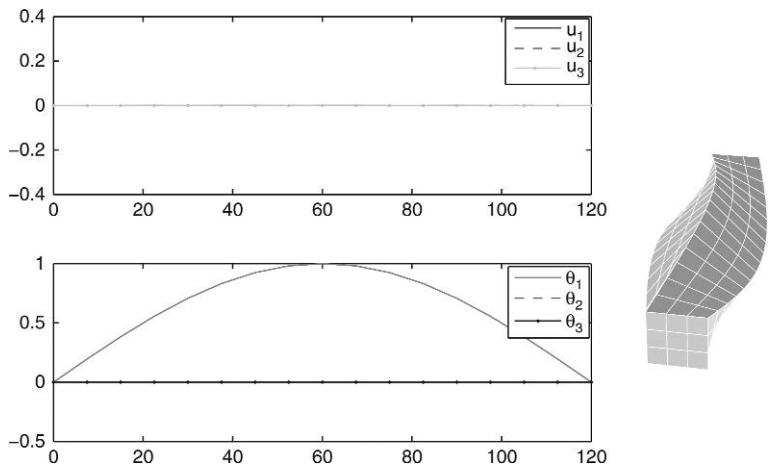

FIG. 4. Straight beam. Vibration mode of frequency ω_2. Displacements and rotations (left). Deformed beam (right).

Figures 7–9 show the lowest frequency vibration modes. The first one is a typical spring mode, the second one is an extensional mode and the third one is a kind of 'phone rope' vibration mode.

4.3 *Test 3: a rod with principal axes not coinciding with the Frenet basis*

The aim of this test is to apply the finite-element method to a rod in which the Frenet basis is not a set of principal axes, so that the off-diagonal term of the inertia matrix $\boldsymbol{I_{nb}}$ does not vanish (see Remark 2.1). With this purpose, we have considered a semicircular rod clamped at both ends, with radius of the centroids line $R = 50\,\text{cm}$ (curvature: $\kappa = 1/R$, torsion: $\tau = 0$, length: $L = \pi R$). The cross-section of the rod is the parallelogram S shown in Fig. 10. In this case $d = 0.025$.

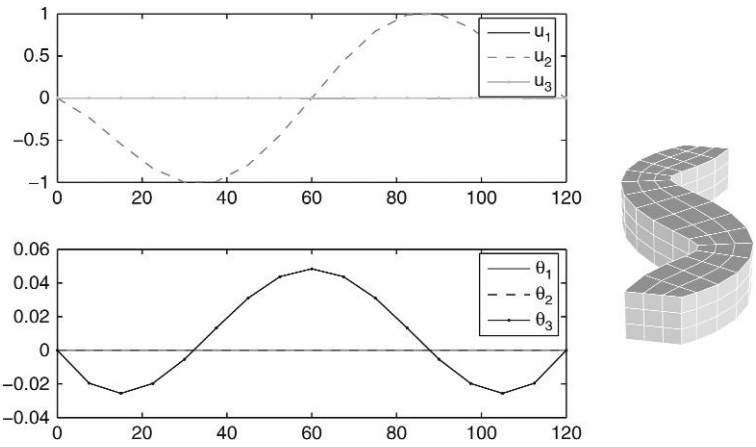

FIG. 5. Straight beam. Vibration mode of frequency ω_3. Displacements and rotations (left). Deformed beam (right).

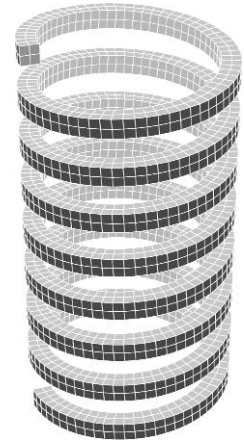

FIG. 6. Undeformed helical rod.

TABLE 2 *Angular vibration frequencies of a helical rod*

Mode	$N = 1024$	$N = 2048$	$N = 3072$	$N = 4096$	Order	ω_{ex}
ω_1^h	15.9146	15.9104	15.9096	15.9094	1.97	15.9090
ω_2^h	18.2507	18.2497	18.2495	18.2494	1.94	18.2493
ω_3^h	19.0345	18.9807	18.9707	18.9672	1.99	18.9626
ω_4^h	19.2888	19.2359	19.2260	19.2226	1.99	19.2181
ω_5^h	31.4845	31.4813	31.4807	31.4805	1.97	31.4802
ω_6^h	35.5888	35.4752	35.4540	35.4466	1.99	35.4369

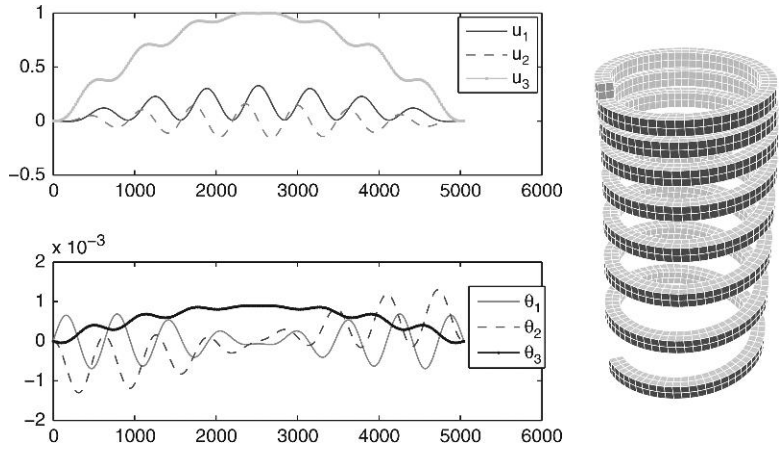

FIG. 7. Helical rod. Vibration mode of frequency ω_1. Displacements and rotations (left). Deformed helix (right).

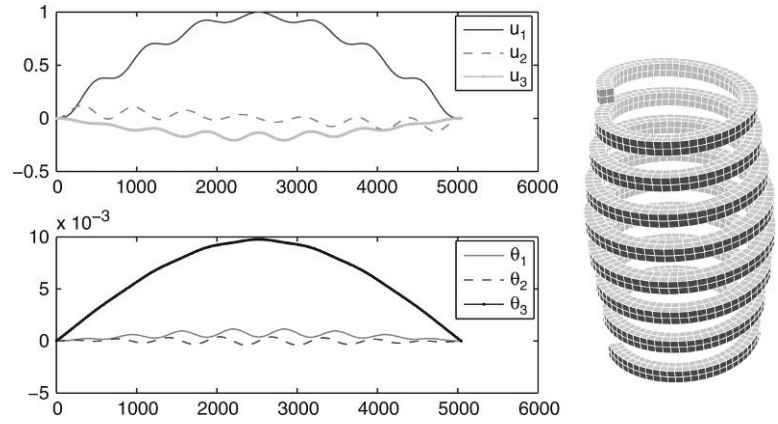

FIG. 8. Helical rod. Vibration mode of frequency ω_2. Displacements and rotations (left). Deformed helix (right).

Figure 11 shows the undeformed rod, seen from two different observation points.

Table 3 shows the lowest vibration frequencies computed on successively refined meshes. It also includes the computed orders of convergence and the exact vibration frequencies ω_{ex}, obtained again by a least squares fitting.

Figures 12 and 13 show the lowest-frequency vibration modes.

4.4 *Test 4: a free ring*

The aim of this test is to assess the performance of the finite-element method applied to rods subject to boundary conditions different from those used to prove the theoretical results of the previous sections. In particular, we consider a free ring, namely, a circular rod whose centroids line is a whole circle subject to periodical boundary conditions.

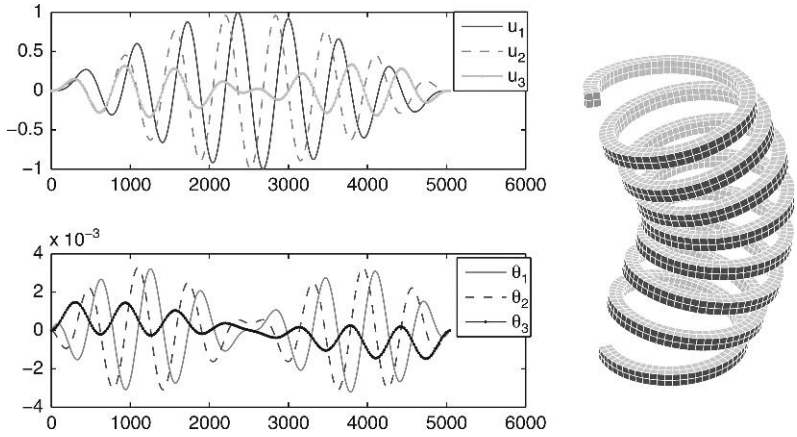

FIG. 9. Helical rod. Vibration mode of frequency ω_3. Displacements and rotations (left). Deformed helix (right).

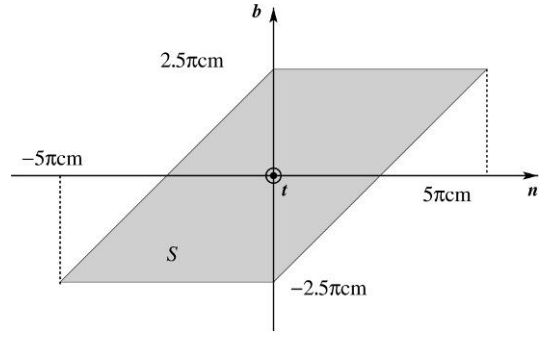

FIG. 10. Cross-section of the semicircular rod.

FIG. 11. Undeformed semicircular rod seen from two observation points.

The radius of the centroids line has been taken again as $R = 50\,\text{cm}$ (curvature: $\kappa = 1/R$, torsion: $\tau = 0$, length: $L = 2\pi R$) and the cross-section a square of side length $b = 5\pi$ cm. Hence, $d = 0.0204$. Figure 14 shows the undeformed ring.

In this case, 0 is an eigenvalue of the continuous and the discrete problems, both with multiplicity 6. The corresponding eigenspace is in both cases the set of admissible rigid motions. Table 4 presents the lowest positive vibration frequencies, computed on successively refined meshes. The table also includes computed orders of convergence and extrapolated exact vibration frequencies ω_{ex} obtained by least squares fitting. Finally, d and s point out whether the vibration frequencies correspond to double or simple eigenvalues, respectively.

TABLE 3 *Angular vibration frequencies of a semicircular rod*

Mode	$N = 32$	$N = 64$	$N = 128$	$N = 256$	Order	ω_{ex}
ω_1^h	836.09	832.71	831.84	831.65	2.00	831.55
ω_2^h	1446.95	1435.02	1432.05	1431.29	2.01	1431.07
ω_3^h	3065.13	3024.53	3014.48	3011.97	2.01	3011.16
ω_4^h	3186.88	3164.30	3158.70	3157.29	2.01	3156.85
ω_5^h	5359.50	5252.03	5225.64	5219.10	2.02	5216.94
ω_6^h	6072.41	6011.77	5996.62	5992.80	2.00	5991.55

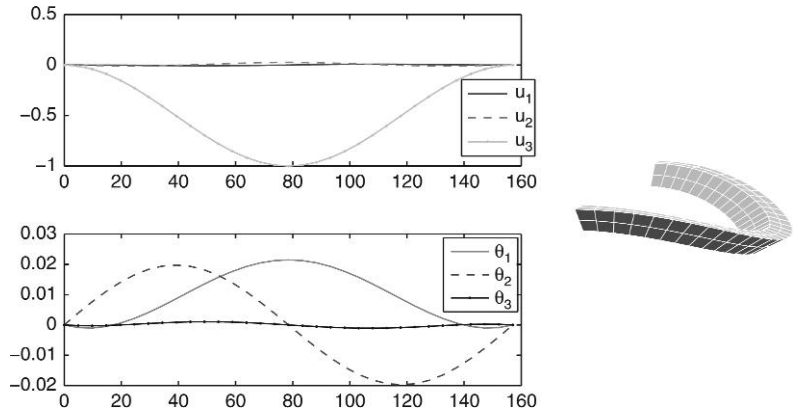

FIG. 12. Semicircular rod. Vibration mode of frequency ω_1. Displacements and rotations (left). Deformed rod (right).

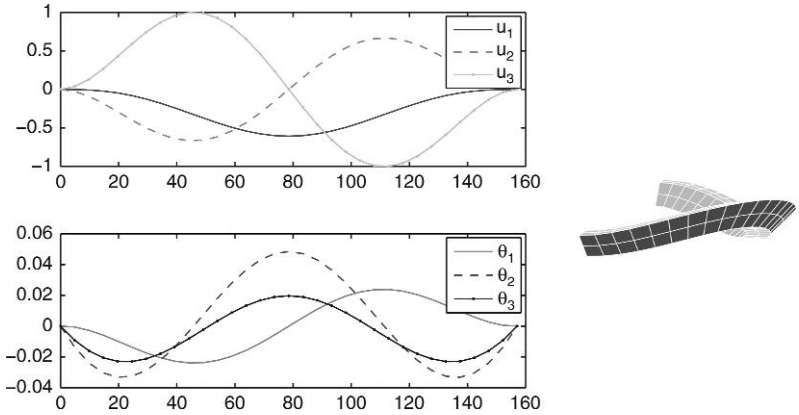

FIG. 13. Semicircular rod. Vibration mode of frequency ω_2. Displacements and rotations (left). Deformed rod (right).

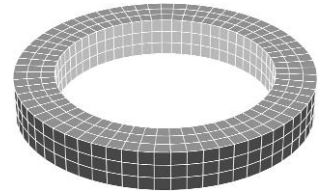

FIG. 14. Undeformed ring.

TABLE 4 *Angular vibration frequencies of a free ring*

Mode	$N = 64$	$N = 128$	$N = 256$	$N = 512$	Order	ω_{ex}	d/s
ω_1^h	2310.12	2294.90	2291.12	2290.15	2.00	2289.83	d
ω_2^h	2371.63	2358.77	2355.54	2354.73	2.00	2354.48	d
ω_3^h	6255.36	6195.63	6180.79	6177.06	2.01	6175.84	d
ω_4^h	6345.58	6288.95	6274.89	6271.38	2.01	6270.23	d
ω_5^h	7241.09	7241.09	7241.09	7241.09	—	7241.09	s
ω_6^h	9532.42	9531.20	9530.89	9530.79	2.00	9530.79	d
ω_7^h	10240.41	10240.41	10240.41	10240.41	—	10240.41	s
ω_8^h	11305.06	11147.82	11108.91	11099.20	2.01	11095.98	d

It can be seen from Table 4 that the computed fifth and seventh vibration frequencies coincide for all meshes. The fifth one corresponds to a purely torsional mode: a constant rotation with respect to the tangential vector. For this mode, θ_1 is constant and θ_2, θ_3 and all the components of $\boldsymbol{u}$ vanish (see Fig. 17 below). On the other hand, the seventh mode corresponds to a constant radial expansion of the whole ring, for which u_2 is constant and u_1, u_3 and $\boldsymbol{\theta}$ vanish. In both cases, the vibration modes can be exactly represented in the finite-element space for any mesh. This is the reason why the computed results are exact, even for the coarser meshes.

Figures 15–17 show some of the vibration modes.

4.5 *Test 5: assessing the locking-free property of the method*

The aim of this final test is to assess the performance of the finite- element method as the nondimensional thickness parameter d approaches zero. With this purpose, we have computed the lowest frequency vibration modes for several rods, all with identical geometrical parameters, except for d, which takes different values approaching zero.

We have considered again a helix clamped at both ends. The centroids line is given by 4.1, now with $A = 100\,\text{cm}$ and $C = 100\,\text{cm}$ (curvature: $\kappa = A/n^2$, torsion: $\tau = C/n^2$). The length of the helix has been taken as $L = \pi n$, which corresponds to half a turn. The section is a square of side length chosen so that the parameter d varies from 10^{-1} to 10^{-4}. Figure 18 shows the undeformed helix for $d = 0.02$.

Tables 5 and 6 show the lowest computed rescaled eigenvalues $\lambda_h^{(j)} := (\omega_j^h)^2\rho/d^2$ ($j = 1$ and 2, respectively) for different values of d and successively refined meshes. According to Lemma 2.6 and

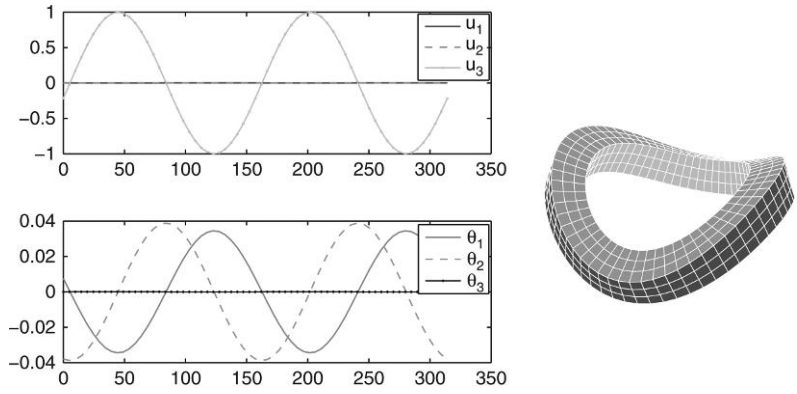

FIG. 15. Free ring. Vibration mode of frequency ω_1. Displacements and rotations (left). Deformed rod (right).

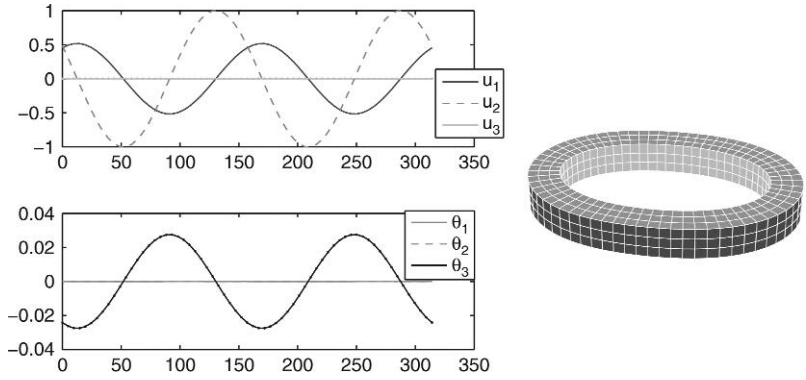

FIG. 16. Free ring. Vibration mode of frequency ω_2. Displacements and rotations (left). Deformed rod (right).

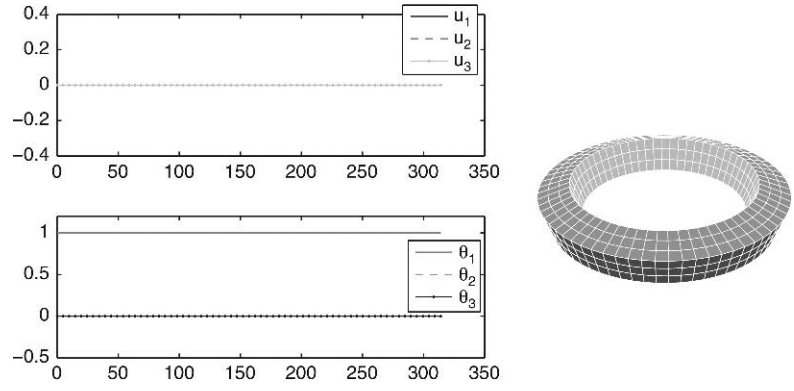

FIG. 17. Free ring. Vibration mode of frequency ω_5. Displacements and rotations (left). Deformed rod (right).

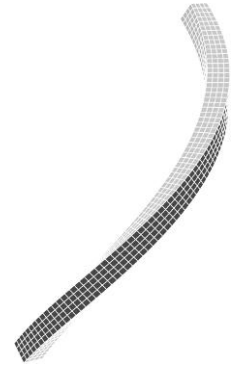

FIG. 18. Undeformed helical rod.

TABLE 5 *Lowest rescaled eigenvalue* $\lambda_h^{(1)} \times 10^{-6}$ *for helical rods of different thickness*

d	$N = 32$	$N = 64$	$N = 96$	$N = 128$	Order	$\lambda_{\text{ex}} \times 10^{-6}$	C
10^{-1}	1.2706	1.2618	1.2602	1.2596	2.00	1.2589	60.76
10^{-2}	2.0568	2.0374	2.0339	2.0326	2.01	2.0310	130.34
10^{-3}	2.0702	2.0506	2.0470	2.0457	2.01	2.0442	131.32
10^{-4}	2.0704	2.0508	2.0472	2.0459	2.01	2.0443	131.32

TABLE 6 *Second lowest rescaled eigenvalue* $\lambda_h^{(2)} \times 10^{-6}$ *for helical rods of different thickness*

d	$N = 32$	$N = 64$	$N = 96$	$N = 128$	order	$\lambda_{\text{ex}} \times 10^{-6}$	C
10^{-1}	3.5180	3.4862	3.4803	3.4783	2.00	3.4756	219.5
10^{-2}	13.8379	13.5438	13.4900	13.4712	2.02	13.4475	1920.8
10^{-3}	14.1715	13.8673	13.8116	13.7922	2.02	13.7677	1987.4
10^{-4}	14.1749	13.8706	13.8149	13.7954	2.02	13.7709	1988.4

Theorem 3.7, as d and h go to zero, $\lambda_h^{(j)}$ should converge to the corresponding rescaled eigenvalues of the limit problem. This can be clearly observed in both tables. The tables also include the computed orders of convergence t and the exact rescaled eigenvalue λ_{ex} obtained by means of a least squares fitting of the model

$$\lambda_h^{(j)} \approx \lambda_{\text{ex}} + Ch^t.$$

We also include in these tables the fitted value of the constant C, in order to show that it does not deteriorate as the thickness parameter becomes small (indeed, clearly C also converges as d goes to zero). This confirms that the method is locking-free.

5. Conclusions

We have analysed the problem of computing the vibration modes and frequencies of a Timoshenko rod of arbitrary geometry. With this purpose, we have considered a finite-element mixed method of arbitrary order, based on that proposed by Arunakirinathar and Reddy for the corresponding load problem. The geometrical assumptions for our analysis are slightly more general; in particular, we have not assumed that the Frenet basis determined by the centroids line of the rod is a set of principal axes.

We have proved optimal order of convergence for displacements, rotations and shear stresses of the eigenfunctions, as well as a double order for the vibration frequencies. We have also proved that the method is locking-free; namely, the convergence does not deteriorate as the thickness of the rod becomes small.

We have implemented the lowest-order method and reported several numerical experiments, which allow us to assess the performance and robustness of this approach. In all cases, the theoretically predicted optimal order of convergence ($\mathcal{O}(h^2)$ for the vibration frequencies) has been attained. This happens even in cases of boundary conditions not covered by the theoretical analysis. Moreover, the experiments show that the method is thoroughly locking-free.

Funding

FONDECYT (1070276 to E.H.); USM (12.05.26 to E.H., E.O.); FONDAP in Applied Mathematics to R.R.; CONICYT to F.S.

References

ARNOLD, D. N. (1981) Discretization by finite elements of a model parameter dependent problem. *Numer. Math.*, **37**, 405–421.

ARUNAKIRINATHAR, K. & REDDY, B. D. (1993) Mixed finite element methods for elastic rods of arbitrary geometry. *Numer. Math.*, **64**, 13–43.

BABUŠKA, I. & OSBORN, J. (1991) Eigenvalue problems. *Handbook of Numerical Analysis* (P. G. Ciarlet & J. L. Lions eds), vol. 2. Amsterdam: North Holland, pp. 641–687.

BABUŠKA, I. & SURI, M. (1992) On locking and robustness in the finite element method. *SIAM J. Numer. Anal.*, **29**, 1261–1293.

BOFFI, D., BREZZI, F. & GASTALDI, L. (1998) On the convergence of eigenvalues for mixed formulations. *Ann. Scuola Norm. Sup. Pisa Cl. Sci.*, **25**, 131–154.

BOFFI, D., BREZZI, F. & GASTALDI, L. (2000) On the problem of spurious eigenvalues in the approximation of linear elliptic problems in mixed form. *Math. Comput.*, **69**, 121–140.

BREZZI, F. & FORTIN, M. (1991) *Mixed and Hybrid Finite Element Methods.* New York: Springer.

CHAPELLE, D. (1997) A locking-free approximation of curved rods by straight beam elements. *Numer. Math.*, **77**, 299–322.

DURÁN, R., HERNÁNDEZ, E., HERVELLA-NIETO, L., LIBERMAN, E. & RODRÍGUEZ, R. (2003) Error estimates for low-order isoparametric quadrilateral finite elements for plates. *SIAM J. Numer. Anal.*, **41**, 1751–1772.

DURÁN, R., HERVELLA-NIETO, L., LIBERMAN, E., RODRÍGUEZ, R. & SOLOMIN, J. (1999) Approximation of the vibration modes of a plate by Reissner–Mindlin equations. *Math. Comput.*, **68**, 1447–1463.

HUANG, T. C. (1961) The effect of rotatory inertia and of shear deformation on the frequency and normal mode equations of uniform beams with simple end conditions. *J. Appl. Mech.*, **28**, 579–584.

KARAMI, G., FARSHAD, M. & YAZDCHI, M. (1990) Free vibrations of spatial rods—a finite-element analysis. *Commun. Appl. Numer. Methods*, **6**, 417–428.

KATO, T. (1995) *Perturbation Theory for Linear Operators.* Berlin: Springer.

KIKUCHI, F. (1982) Accuracy of some finite element models for arch problems. *Comput. Methods Appl. Mech. Eng.*, **35**, 315–345.

LITEWKA, P. & RAKOWSKI, J. (2001) Free vibrations of shear-flexible and compressible arches by FEM. *Int. J. Numer. Methods Eng.*, **52**, 273–286.

LOULA, A. F. D., FRANCA, L. P., HUGHES, T. J. R. & MIRANDA, I. (1987) Stability, convergence and accuracy of a new finite element method for the circular arch problem. *Comput. Methods Appl. Mech. Eng.*, **63**, 281–303.

REDDY, B. D. (1988) Convergence of mixed finite element approximations for the shallow arch problem. *Numer. Math.*, **53**, 687–699.

REDDY, B. D. & VOLPI, M. B. (1992) Mixed finite element methods for the circular arch problem. *Comput. Methods Appl. Mech. Eng.*, **97**, 125–145.